

Titre: Condition monitoring and diagnostic of rotating machinery by means of wavelet transforms
Title:

Auteurs: M. S. Safizadeh, Aouni A. Lakis, & M. Thomas
Authors:

Date: 1999

Type: Rapport / Report

Référence: Safizadeh, M. S., Lakis, A. A., & Thomas, M. (1999). Condition monitoring and diagnostic of rotating machinery by means of wavelet transforms. (Technical Report n° EPM-RT-99-07). <https://publications.polymtl.ca/10179/>
Citation:

Document en libre accès dans PolyPublie

Open Access document in PolyPublie

URL de PolyPublie: <https://publications.polymtl.ca/10179/>
PolyPublie URL:

Version: Version officielle de l'éditeur / Published version

Conditions d'utilisation: Tous droits réservés / All rights reserved
Terms of Use:

Document publié chez l'éditeur officiel

Document issued by the official publisher

Institution: École Polytechnique de Montréal

Numéro de rapport: EPM-RT-99-07
Report number:

URL officiel:
Official URL:

Mention légale:
Legal notice:

21 MAI 1999

**CONDITION MONITORING AND DIAGNOSTIC
OF ROTATING MACHINERY BY MEANS OF
WAVELET TRANSFORMS**

By

M.S. SAFIZADEH, A.A. LAKIS and M. THOMAS

Department of Mechanical Engineering
École Polytechnique de Montréal

1999

No. EPM/RT-99/7

gratuit

LEGENDS OF FIGURES

- Figure 1: Comparison between Fourier transform and Wavelet transform.
- Figure 2: Haar wavelet and its Fourier spectrum.
- Figure 3: Morlet wavelet and its Fourier spectrum.
- Figure 4: Mexican-hat wavelet and its Fourier spectrum.
- Figure 5: Meyer Wavelet function.
- Figure 6: Lemarie-Battle wavelet function.
- Figure 7: Daubechies wavelet function.
- Figure 8: (a) Dyadic sampling grid in the time-scale plane
(b) Time-frequency plane of the Short-Time Fourier Transform
(c) Time-frequency plane of the wavelet transform
- Figure 9: (a) Subband coding scheme H: high pass filter and G: low pass filter
(b) Filter bank tree of the discrete wavelet transform
- Figure 10: Filter bank tree of the wavelet packet transform.
- Figure 11: Block diagram of the “zoom in wavelet transform”.
- Figure 12: (a) Time representation of the sum of sine waves
(b) The wavelet transform of the sum of sine waves by Daubechies filter (D20)
(c) The wavelet transform of the sum of sine waves by Daubechies filter (D2)
- Figure 13: Wavelet packet transform of a sum of sine waves.
- Figure 14: Time-frequency representation of a sum of sines wave by the Gabor dictionary.
- Figure 15: Wavelet transform of a Dirac function.
- Figure 16: Wavelet packet transform of a Dirac function.
- Figure 17: Time-frequency representation of a Dirac function by the Gabor dictionary.

- Figure 18: Wavelet transform and mean-square wavelet map of an amplitude-modulated sine.
- Figure 19: Wavelet packet transform and mean-square wavelet packet map of an amplitude-modulated sine.
- Figure 20: Time-frequency representation of an amplitude-modulated sine by the Gabor dictionary.
- Figure 21: Wavelet transform and mean-square wavelet map of a frequency-modulated sine.
- Figure 22: Wavelet packet transform and mean-square wavelet packet map of a frequency-modulated sine.
- Figure 23: Time-frequency representation of a frequency-modulated sine by the Gabor dictionary.
- Figure 24: Test setup.
- Figure 25: Wavelet transform and mean-square wavelet map of the measured signal on a defective bearing.
- Figure 26: Wavelet packet transform and mean-square wavelet packet map of the measured signal on a defective bearing.
- Figure 27: Wavelet transform and mean-square wavelet map of the de-noised signal of the defective bearing.
- Figure 28: Wavelet packet transform and mean-square wavelet packet map of the de-noised signal of the defective bearing.
- Figure 29: Wavelet transform and mean-square wavelet map of the signal measured on a defective gearbox.
- Figure 30: Wavelet packet transform and mean-square wavelet packet map of the signal measured on a defective gearbox.
- Figure 31: Time-frequency representation of the signal measured on a defective gearbox by the Gabor dictionary.
- Figure 32: Zoom in wavelet transform of the signal measured on a defective gearbox between the frequency band 320 Hz and 640 Hz.

ABSTRACT

Time-frequency analysis has been found to be effective in monitoring the transient or time-varying characteristics of machinery vibration signals, and therefore its use in machine condition monitoring is increasing. While the short-time Fourier transform and the Wigner-Ville distributions are generally considered satisfactory in the field of time-frequency analysis, the development of such new techniques as wavelet analysis, by which it is possible to compensate for weaknesses in other time-frequency methods, may lead to new solutions to unsolved problems. Wavelet analysis has a special characteristic of time-frequency localization, which is very effective in the analysis of transient or time-varying signals. In this paper, we present a brief study of the wavelet transform, wavelet functions, the discrete wavelet transform, the wavelet packet transform and adaptive wavelet transforms. Examples are given to show the advantages and disadvantages of different wavelet transforms. Finally, the effectiveness of wavelet analysis in condition monitoring and diagnostics of machines is illustrated by experimental results from a defective bearing, followed by the application of this technique to the detection of a broken tooth in a gearbox.

1. INTRODUCTION

A diagnosis is not an assumption, it is a conclusion reached after a logical evaluation of the observed symptoms. The diagnostic process includes the following steps:

- a) Observation of the different symptoms and determination of the various defects in the machinery which may have caused them;
- b) A systematic search for possible defects in the measured signals;
- c) Evaluation of various hypotheses and determination of the one which is compatible with all apparent symptoms.

The diagnosis, therefore, is based on the systematic analysis of the symptoms found in the measured signals.

The key factor is the signal analysis. A great many indicators have been developed for machine condition monitoring and fault detection, such as the crest factor and Kurtosis. Comparing new reading against published severity chart such as VDI 2056 shows the existence of defaults.

Machine monitoring and/or diagnosis on the basis of variations in the indicator values of the signal spectrum in "large bands" and in "narrow bands" is very unreliable. One reason for this is that it is necessary to define a large number of indicators corresponding to a small number of defects.

In addition, we need to take into consideration not only the increase in the power of the signal, but also the development of its form. Analysis of this development is carried out in the frequency domain (diagnosis by comparison of the spectrums).

On the other hand, the identification of tooth comb parts in high frequency by traditional spectrum analysis

is often impossible, since the frequencies of these components correspond to very high orders of the rotation frequency, and all fluctuations in the rotation frequency produce important frequency variations in each of the components by sweeping across several spectral lines. The spectrum obtained in this way is very noisy and it is difficult to determine the repetitive frequencies of the shocks.

Modifications to the form of representation of the signal, such as Cepstrum (the inverse Fourier transform of the logarithmic spectrum of the signal) and the Hilbert transform of the narrow band of the signal, reveal further information. Here, we are dealing with non-stationary or cyclo-stationary events in the time domain. Advanced signal processing techniques are required to enable us to represent the signal in three dimensions (time-frequency-amplitude). These techniques permit us:

- a) To detect and follow the development of the defects which generate weak vibrational power. However, the weak vibrational power can modify the form of the signal to a considerable extent, as happens when defects produce the amplitude modulation or frequency modulation of certain characteristic components. Examples of this are the journal bearing of a shaft with a slow or very slow rotational velocity, a rotating oven, dryer cylinders, the press sections of a paper machine, etc.;
- b) To supervise the installations in which the normal functional process produces high amplitude periodic shocks (piston or screw compressor, reciprocating machinery [1] and cam mechanisms [2], ...) which may mask the faulty frequency producing the impulsive forces. (fault in a bearing, coupling, ...).

The time-frequency methods are regarded as advanced diagnostic techniques which offer high sensitivity

to faults and a good diagnostic capability.

The Short-Time Fourier Transform (STFT) is one method of time-frequency analysis which we have studied [3]. In the STFT, signal is cut by a window with length T and centered at time t ; the spectrum coefficients are calculated for this portion of the signal. The window is then moved to a new position and so on. The major drawback of the STFT is the fixed-length of the window (T) during the analysis of the signal. This limitation of the STFT creates the fundamental problem of the STFT, namely that high resolution can not be obtained simultaneously in the time and frequency domains. If the window length is T , then its frequency bandwidth is of the order $1/T$ (because of $BT=1$). Thus, the two conditions of a narrow window and a narrow bandwidth are irreconcilable.

Another time-frequency method which we have studied [4] are the Wigner-Ville distributions. In this case, it is postulated that a series of sampled data is available for analysis. The instantaneous correlation, $R_f(\tau, t_1)$, at time (t_1) with a time lag τ , is defined as

$$R_f(\tau, t_1) = \lim_{T \rightarrow \infty} \int_{t_1}^{t_1 + \tau} f(t - \frac{\tau}{2}) f(t + \frac{\tau}{2}) dt \quad (1)$$

and its Fourier transform may be written as follows:

$$S_f(\omega, t_1) = \int_{-\infty}^{\infty} R_f(\tau, t_1) e^{-j\omega\tau} d\tau \quad (2)$$

Where $S_f(\omega, t_1)$ is the instantaneous spectrum density function according to frequency ω and time t_1 .

Theoretically, $S_f(\omega, t_1)$ is the frequency content measurement of a non-stationary random process at time t_1 .

In practice, it is impossible to calculate the correlation function $R_f(\tau, t_1)$ on a series of samples from $-\infty$

to $+\infty$, because this type of sample is never available.

Therefore, if we replace:

$$\int_{t_1}^{t_1+\tau} f(t-\frac{\tau}{2}) f(t+\frac{\tau}{2}) d\tau$$

in the equation (2), by the instantaneous value: $f(t-\frac{\tau}{2})f(t+\frac{\tau}{2})$ we will obtain

$$W_f(\omega, t) = \int_{-\infty}^{\infty} f(t-\frac{\tau}{2}) f(t+\frac{\tau}{2}) e^{-j\omega\tau} d\tau \quad (3)$$

$W_f(\omega, t)$ is a function of ω and t for a sampled single x and is called the Wigner Distribution of $f(t)$.

In the case of deterministic signals, we use the analytical signal $z(t)$ instead of the real signal $f(t)$, and the distribution is called the Wigner-Ville Distribution. The analytical signal $z(t)$ is defined as

$$z(t) = f(t) + j \bar{f}(t) \quad (4)$$

Where $\bar{f}(t)$, the imaginary part of the signal $z(t)$, is the Hilbert transform of the real signal $f(t)$.

In this way, the negative frequencies are eliminated and the signal is represented only by the real part of a rotary phaser with positive frequencies.

The analytical signal is very useful when we study the amplitude and modulation of the phase since this signal introduces the concept of instantaneous frequency and instantaneous power. The sampling frequency may also be used, followed by the Nyquist criteria because the spectrum of an analytical signal is a one-sided spectrum with only positive frequencies.

The Wigner-Ville Distribution is a distribution of energy in the time and frequency domains, where:

$$E_s = \int \int WVD_f(\omega, t) dt d\omega \quad (5)$$

Unfortunately, the Wigner-Ville transform presents several anomalies:

- a) This transform is a bilinear transform i.e. the cross terms generate a certain non-linearity;
- b) The random noise in the original signal has a tendency to spread to other regions in the time domain. Since the integral of equation (3) is centered at time t , the integral covers an infinite period of τ (time delay). Therefore, it depends on the characteristics of x as distinct from the local time t ;
- c) These transforms often give negative values, which makes the interpretation of the distribution difficult.

Furthermore, the Wigner-Ville method presents another difficulty: it is almost impossible to obtain a local spectrum density because of the continuity nature of the harmonic waves. To overcome this limitation attributable to harmonic analysis, an alternative method of signal analysis has, at a theoretical level, been developed:

Instead of using sines and cosines as base functions to decompose a signal, a set of orthogonal functions, called wavelets, has been used. Whilst, by definition, harmonic functions go to infinity, the wavelets are, in contrast, local functions. Gathering these wavelets and using different scales, it is possible to assemble a set of base functions in order to examine the local character of non-stationary signals.

The theory of wavelets is a mathematical method in which a series of special signals is used to construct a model for a signal, a system or a process. These special signals are small waves or wavelets. They must be oscillatory and possess an amplitude which decreases rapidly to zero in both positive and negative

directions.

The first classical wavelet was derived by J. Morlet [5], a geophysical engineer at a French oil company, in 1982. He wanted to analyse some signals which had shorter-time transient components in high frequency than in low frequency. He needed both satisfactory frequency resolution in low frequency and satisfactory time resolution in high frequency. The usual method of time-frequency analysis at that time was the Short-Time Fourier Transform (STFT). As previously mentioned, the major disadvantage of the STFT is that it is impossible to obtain high resolution simultaneously in time and in frequency. Morlet's idea was to use a smooth window with some oscillations, as $\psi(t)$ in Figure. 3, and generate a label family from $\psi(t)$ by translation and dilation. As a basis for the wavelet transform, he chose a windowed cosine wave which was compressed in time for a higher frequency function and spread out for a low frequency function. He finally characterized his signal by inner products of the signal with these transform functions. A few years later, Alex Grossmann, a theoretical physicist, presented an exact inversion of Morlet's formula and helped him to find several applications for the wavelet transform [6]. In 1985, Y. Meyer, a pure mathematician, recognized that the wavelet transform had been already introduced as a mathematical tool in harmonic analysis by Calderon in the 1960s. He correlated the work of Grossmann and Morlet with Calderon's formula in harmonic analysis and also constructed the basis of an orthonormal wavelet with excellent time-frequency localization properties. In 1986, S. Mallat, a specialist in computer vision and image processing, used the multi-resolution approaches in computer vision and its application to a method of image coding called "Pyramid", in order to define a similar structure for wavelet expansions. Mallat and Meyer succeeded in developing the mathematical structure for wavelet construction on the basis of multi-resolution

signal representation [7, 8]. Meyer's work on the mathematical structure of the wavelet is documented in his book [9]. Using multi-resolution analysis, S. Mallat proposed that the wavelet coefficients may be computed using an efficient algorithm produced by a filter bank. To use filters in wavelet decomposition instead of deriving the filters from a wavelet basis, we can first construct a pair of appropriate FIR (finite impulse response) filters and then investigate whether they correspond to an orthonormal wavelet basis. The characteristics of such a pair of filters were discovered in 1970 and given the name "quadrature mirror filters" (QMF). By using QMF, exact construction of orthonormal wavelet bases has been possible. A sufficient condition for regularity of these filters has been given by Daubechies [10, 11]. This work resulted in a discrete-time wavelet transform [12, 13]. One of the important disadvantages of the wavelet transform is the logarithmic scale of the frequency axis in the time-frequency plane. As an alternative, an interesting generalization of the filter bank trees of the wavelet transform is the wavelet packets transform, which provides a linear scale frequency axis in the time-frequency plane [14, 15].

This paper presents the wavelet analysis as a newly-developed technique with important properties which make it a powerful tool in machine condition monitoring and fault detection. In section 2, the theory of wavelet transform is briefly described, followed by a discussion of the properties of different wavelet functions. Then, the discrete wavelet transform and the fast wavelet transform based on multi-resolution analysis are studied and the wavelet packet transform and adaptive wavelet transforms are presented as variations of wavelet analysis. In this section, we also present a new method, called the "zoom in wavelet transform", by means of which the wavelet transform is used to obtain a finer resolution in the frequency domain. This method is a variation of the adaptive wavelet transform. In section 3, a computer program to implement the different methods of wavelet analysis is described and the different ways of using the

wavelet transform to determine time-frequency localization are compared. Finally, wavelet analysis is applied to experimental vibration signals received from a damaged bearing and a broken tooth in a gearbox.

2. WAVELET TRANSFORMS

It is known that discrete-time signal decompositions are methods of expressing an energy-limited signal as a linear combination of transform bases. The linear integral transforms can be considered as an inner product of a signal $f(t)$ with a transformation function. The standard example is the Fourier transform

$F_f(\omega)$ of signal $f(t)$ which is defined as:

$$F_f(\omega) = \langle f, h \rangle = \int_{-\infty}^{\infty} f(t) \bar{h}(t) dt \quad (6)$$

where the transformation kernel is $h(t) = e^{i\omega t}$.

From a mathematical point view, equation (6) decomposes $f(t)$ into a family of pure frequency signals $e^{i\omega t}$ which play the role of the Fourier transform bases. The sine-cosine functions are highly localized in frequency but widely spread in time. Therefore, the time domain information of the spectral components is hidden in the phase of the Fourier transform. Consequently, the Fourier transform is not well suited for time-place analysis.

For non-stationary signals, the Short-Time Fourier Transform (STFT) is the first and simplest method which is defined as

$$STFT_f(t, \omega) = \langle f, h_\tau \rangle = \int_{-\infty}^{\infty} f(t) \bar{h}_\tau(t) dt \quad (7)$$

where $h_\tau(t) = g(t - \tau) e^{i\omega t}$ and τ define the translation of the window function $g(t)$. As the window is shifted in time, a new spectrum is obtained at each position, producing a time-frequency representation of the signal. The efficiency of the localization in the time-frequency plane depends on the width of the window function. The uncertainty factor, $\Delta t \Delta \omega \geq 1/2$, sets a limit on the product of time and frequency. This means that we cannot simultaneously obtain high resolution in both the time and frequency domains. However, by changing the width of the window, we can trade resolution in time for resolution in frequency. In a similar way, the wavelet transform can be defined if the Fourier transform bases are replaced by the wavelet transform bases, $h_{s\tau}(t)$, as shown in Figure 1.

The wavelet transform is defined as:

$$W_f(s, \tau) = \langle f, h_{s\tau} \rangle = \int_{-\infty}^{\infty} f(t) \bar{h}(s, \tau) dt \quad (8)$$

The wavelet transform bases are a family of functions which are obtained from a single prototype wavelet by translation and dilation/contraction :

$$h_{s\tau}(t) = \frac{1}{\sqrt{s}} h\left(\frac{t - \tau}{s}\right) \quad (9)$$

where “ s ” is a real variable, known as the scale of wavelet transform and $h(\cdot)$ is a fixed function, called “mother wavelet function”. From equation (9), we can say that the wavelet transform extracts spectral

information from the signal around time τ by means of inner links between the signal and scaled versions of the wavelet.

In the case of the wavelet transform, the selection of the basis functions is more flexible than the case with the STFT. The choice of short basis functions for low frequencies and long basis functions for high frequencies makes the wavelet transform sharper in time in the higher frequencies and sharper in frequency at low frequencies.

2.1. Wavelet Functions

The mother wavelet function may be any function satisfying the necessary condition that warrants the existence of the inverse wavelet transform. This admissible condition is defined as

$$\int_{-\infty}^{\infty} h(t)dt = 0 \quad (10)$$

which means that the wavelet be oscillated to have a zero mean. Different families of wavelets can be generated by taking different admissible wavelet functions. The choice of the wavelet function is important and rather critical. The selection of the wavelet depends on the characteristics of the signal and on the acceptability of other effects in the representation due to the wavelet function. In the following we review some popular wavelets:

a) Haar Wavelet

The Haar wavelet is the first and the simplest wavelet function which was constructed by Haar in 1910. He was a mathematician who looked for an orthonormal system with the functions

$h_0(x), h_1(x), \dots, h_n(x), \dots$ defined between interval $[0,1]$, such that the series

$$\langle f, h_0 \rangle h_0(x) + \langle f, h_1 \rangle h_1(x) + \dots + \langle f, h_n \rangle h_n(x) + \dots \quad (11)$$

where $\langle u, v \rangle = \int_0^1 u(x)v^*(x)dx$

Haar chose the step function $h(x)$, called Haar's wavelet function, which is defined as:

$$h(x) = \text{rectangle}[2(x - 1/4)] - \text{rectangle}[2(x - 3/4)] \quad (12)$$

which is real and antisymmetric about $t = 1/2$, as shown in Figure 2. For $n \geq 1$, we have

$n = 2^j + k$, $j \geq 0$, $0 \leq k \leq 2^j$, and $h_n(x) = 2^{j/2} h(2^j x - k)$. In this case, the series

$h_0(x), h_1(x), \dots, h_n(x), \dots$ is called an orthonormal base or Hilbertian base of $L^2[0,1]$.

It is easy to show that the functions of the series are orthonormal with respect to the scalar product and they are normalized by the factor $2^{j/2}$. Several years later, it was shown that the Haar base has the multiscale structure which is a prerequisite for wavelet function.

A major disadvantage of Haar's wavelets is the discontinuity of this wavelet which cannot provide a good approximation for smooth functions. The Fourier transform of Haar's wavelet may be written as

$$H(f) = 2i \exp(-i\pi f) \frac{1 - \cos \pi f}{\pi f} \quad (13)$$

The decay of the Haar wavelet is very slow. Figure 2 shows Haar's wavelet and its Fourier spectrum.

b) Morlet Wavelet

This wavelet is in essence a Gaussian modulated harmonic function which was used by J. Morlet for the analysis of sound patterns:

$$h(t) = \exp(i2\pi f_0 t) \exp\left(-\frac{t^2}{2}\right) \quad (14)$$

Its real part is an even cos-Gaussian function. The Fourier transform of the Morlet wavelet is the Gaussian functions shifted to f_0 and $-f_0$:

$$H(f) = 2\pi \left\{ \exp[-2\pi^2 (f - f_0)^2] + \exp[-2\pi^2 (f + f_0)^2] \right\} \quad (15)$$

which is even and real positive valued. This wavelet does not satisfy the admissible condition, because

$H(0) \geq 0$. In practice, one often chooses f_0 so that the ratio of the highest and the second highest

maximum of $h(t)$ is approximately 1:2, i.e. $2\pi f_0 \approx 5$. In this case, the value of $H(0)$ is very close to

zero, i.e. $H(0) = 3.7 \times 10^{-6}$. Here, it can be considered as zero with a good approximation.

By this wavelet, the analysis is not orthogonal. The real part of the $h(t)$ and its Fourier spectrum are

shown in Figure 3.

c) Mexican-hat Wavelet

This wavelet is in fact the second derivative of the Gaussian function which is introduced by Gabor.

$$h(t) = (1 - |t|^2) \exp\left(-\frac{|t|^2}{2}\right) \quad (16)$$

It is even and real valued. The Fourier transform of the Mexican-hat wavelet is

$$H(f) = 4\pi^2 f^2 \exp(-2\pi f^2) \quad (17)$$

which is even and real valued, as shown in Figure 4. The decay of the wavelet coefficient is fast. This wavelet has been applied in vision analysis.

d) Meyer Wavelet

Y. Meyer is a pure mathematician who constructed an orthonormal wavelet basis with excellent time-frequency localization properties in 1985. The Meyer wavelet is defined in the frequency domain as

$$H(f) = \exp(-i\pi f) \sin[v(f)] \quad (18)$$

which $v(f)$ is a symmetric function defined by

$$\begin{cases} v(1-f) = \frac{\pi}{2} - v(f) & \text{for } 1/3 \leq f \leq 2/3 \\ v(2f) = \frac{\pi}{2} - v(f) & \text{for } 1/3 \leq f \leq 2/3 \end{cases} \quad (19)$$

The Meyer wavelets in the time domain can be written as follows:

$$h(t) = 2 \int_0^\infty \sin[v(f)] \cos[2\pi(t - 1/2)f] df \quad (20)$$

One can easily check that it is a real symmetric function at $t = 1/2$. By changing the auxiliary function

$v(f)$, we obtain a different family of wavelets. Although the Meyer wavelet shows rapid polynomial decay, it has wide support. This wavelet is also infinitely differentiable.

The Meyer wavelet for $v(x) = x^4(35 - 84x + 70x^2 - 20x^3)$ is shown in Figure 5.

e) Lemarie-Battle's Wavelets

Lemarie was a student of Meyer who worked in harmonic analysis and Battle was a mathematical physicist who was interested in quantum field theory. Independently of one another, they developed wavelet bases consisting of spline functions. An explicit expression for this wavelet family does not exist and the properties of each member of the family can be different and depend on the choice of the spline function. For a constant spline, the wavelets become similar to Haar wavelets. More detail for constructing filters using this wavelet family may be found in [11].

Although the wavelets have exponential decay which is an improvement over the decay of the Meyer wavelet, they lose regularity and are not compactly supported. One of the wavelets is shown in Figure 6.

f) Daubechies Wavelets

Apart from the Haar wavelet function, almost all the orthonormal wavelet functions listed above consist of infinitely supported functions. One desirable property is to have a wavelet with compact support in the time domain, i.e., it is time limited in that it is non-zero only over a given interval. Such a wavelet gives a true sense of time locality. Daubechies constructed a family of orthogonal wavelets which converge to continuous functions with compact support. These wavelets have no explicit expression except for *db1*,

which is the Haar wavelet. The Daubechies family wavelets are real but neither symmetrical nor asymmetrical and their regularity increases as the order of Daubechies' wavelet increases. One member of the Daubechies family ($D4$) is shown in Figure 7. Details of the procedure for constructing an orthonormal base of compactly supported wavelets may be found in Daubechies' original paper [10]. These wavelets have other desirable properties. It can be shown that they are bounded, continuous functions and they are continuously differentiable.

2.2. Discrete Wavelet Transform

In order to apply the wavelet transform for digital signals, the wavelet parameters s, τ must be discretized.

If we consider $s = S_0^m$ and $\tau = nS_0^m T_0$, the corresponding wavelets become:

$$h_{mn}(t) = S_0^{-m/2} \cdot h(S_0^{-m}t - nT_0) \quad (21)$$

$$\text{where } m, n \in \mathbb{Z}, \quad S_0 > 1, \quad T_0 \neq 0$$

This way of discretization may be modified to give a dyadic grid by considering $S_0 = 2, \quad T_0 = 1$;

therefore

$$h_{mn} = 2^{-m/2} \cdot h(2^{-m}t - n) \quad m, n = 1, 2, \dots \quad (22)$$

It is possible to obtain an orthonormal basis for special choices of $h(t)$. The dyadic sampling grid in the time-scale plane is shown in Figure 8(a). The scale axis is often expressed in terms of frequency under transformation $s \rightarrow k/f$ where k is a constant. In fact, it can be shown that the Short-Time Fourier Transform, time-frequency distributions and time-scale methods (wavelet transforms) are members of a

common class of energy representations [16, 8]. A comparison between the basis functions and the time-frequency plane of the Short-Time Fourier Transform (STFT) and those of the wavelet transform is shown in Figure 8(b); the self-adjusting window (zooming) property is the major difference between the wavelet transform and the STFT. The zooming property of the wavelet transform is similar to a microscope or a telescope, where the resolution is automatically adjusted to a different scale of magnification. As shown in Figure 8, the important properties of the wavelet transform, such as its localisability and changeable resolution in the time and frequency domains, make it both more suitable and more effective in the analysis of non-stationary vibration signals such as transients.

The implementation of the wavelet transform according to (22) may only be carried out with some difficulty because, as m increases, $h(t)$ must be sampled at progressively more points. This makes the computations very slow. In 1989, Stephane Mallat [17, 7] proposed an efficient discrete-time algorithm for the computation of the wavelet transform. Mallat, using quadrature mirror filters and multi-resolution analysis, constructed a new algorithm for the computation of the wavelet transform, which calculates the wavelet coefficients very rapidly. It is called the Fast Wavelet Transform and its idea comes from a method called subband coding, which has been used in speech compression. Subband coding, which consists of two branches with filtering followed by down sampling by two, can decompose a signal into two parts. The part that is passed through a low-pass filter gives an approximation of the signal, and the part that is passed through a high-pass filter gives the detail. It is interesting to note that the original signal can be recovered from its two filtered and subsampled parts if the filters have the property of perfect reconstruction, as shown in Figure 9(a). Such filters are called quadrature mirror filters. As shown in

equation (8), a wavelet transform can be interpreted as a decomposition of a signal into a set of frequency channels of different band widths. Mallat's algorithm is a cascade extension of this elementary two-channel filter bank in a binary tree structure, as shown in Figure 9(b).

A review of discrete-time wavelet transform and the relationship between wavelet transform and filter banks is given by Shensa [19], Vetterli et al. [15, 18].

2.3. Wavelet Packet Transform and Adaptive Wavelet Transforms

In wavelet transform, the frequency axis has a logarithmic scale which gives good frequency resolution at lower frequencies and good time resolution in the higher frequencies. For this reason, it is suggested that the wavelet transform be used to analyse signals with long-duration events in the lower frequencies and short-duration events in the higher frequencies.

The generalisation of the discrete-time wavelet transform is called the wavelet packet transform and can be described as a full-tree-structured filter bank, as shown in Figure 10. An interesting advantage of the wavelet packet is that the frequency axis has linear scale which gives better frequency resolution in the higher frequencies, at the price of some loss of time resolution.

It is clear that the wavelet transform is appropriate for signals with transient phenomena in the higher frequencies; however, it may perform less well over other time-frequency transforms. The resolution exchange between time and frequency in the wavelet transform is always fixed and independent of the signal being analysed. This may not be satisfactory in the analysis of an arbitrary class of signals with either unknown or time-varying characteristics. To improve the performance of the wavelet transform, it is necessary to use the signal-adaptive transform, which is more satisfactory than the original fixed transform

although it is important to ensure that this flexibility does not come at too great a cost.

There are two way of achieving this objective:

a) By selecting filter banks to optimize the time and frequency resolutions:

We may select the binary trees in filter banks by taking the characteristics of the signal into account, instead of using the fixed tree of the wavelet transform or the wavelet packet transform [20], as shown in Figure 11. In this way, we can locally exchange resolution in time for resolution in frequency and vice versa.

b) By optimizing the wavelet function with respect to the signal structure:

The second way involves the construction of waveform libraries and the choice of those particular waveforms which are the best adapted for the decomposition of the signal structures. Such waveforms are called time-frequency atoms and the libraries of waveforms are called the dictionary of time-frequency atoms.

One method which follows the idea of searching for good representation from a dictionary of time-frequency atoms is the method of matching pursuit [21]. This method is a linear decomposition of any signal into waveforms that are selected from a dictionary of Gabor functions.

A general family of time-frequency atoms can be generated by scaling ($s > 0$), translating (τ) and frequency modulating (ξ) a single window function $g(t)$.

$$g_{\gamma}(t) = \frac{1}{\sqrt{s}} g\left(\frac{t - \tau}{s}\right) e^{i\xi t} \quad (23)$$

where the index $\gamma = (s, \tau, \xi)$ denotes an element of this family of atoms. The $g(t)$ is the Gaussian

window $g(t) = 2^{1/4} e^{-\pi^2 t^2}$.

Then $f(t)$ can be written

$$f(t) = \sum_{n=-\infty}^{+\infty} a_n g_m(t) \quad (24)$$

where a_n are the expansion coefficients which provide some information on certain types of properties of $f(t)$, depending upon the choice of the atoms $g_m(t)$.

This method is particularly suitable for decomposing signals whose localizations in time and frequency vary widely.

2.4. De-noising

Removing noise from a signal by wavelet analysis is one of the most recent applications of wavelets [22].

The idea of de-noising by wavelet analysis consists of decomposing the signal by wavelet transform, removing noise from components, and reconstructing the signal.

Wavelet analysis is a linear method; therefore the wavelet coefficients of the linear combination of two signals are equal to the linear combination of their wavelet coefficients.

$$W_{(f_1+f_2)} = W_{f_1} + W_{f_2} \quad (25)$$

A noisy signal can be modeled in the following form:

$$f(t) = s(t) + e(t) \quad (26)$$

Where $f(t)$ is a noisy signal, $s(t)$ is the original signal, and $e(t)$ is the noise. Eliminating the noise part of the signal may be done in three following steps:

- a) Compute the wavelet decomposition of the signal $f(t)$
- b) Determine a limit for optimal de-noising and suppress only the portion of the wavelet coefficients that exceeds this limit.
- c) Reconstruct the signal with the help of modified wavelet coefficients $s(t)$.

In practice, the decomposition and reconstruction procedures are accomplished respectively by the fast wavelet transform and the inverse fast wavelet transform.

It is clear that the performance of the de-noising method depends mostly on the step (b). Suppressing a part of a signal, called the thresholding procedure, is carried out using different optimization techniques, which give different threshold values [23]. In next section, we will see how this application of the wavelets can improve the wavelet transform representation of signals.

3. APPLICATION OF THE WAVELET TRANSFORM TO MACHINERY FAULT DIAGNOSIS

The wavelet transform is one of the newer methods of time-frequency analysis that have been used in various science and engineering fields in recent decades. Although the wavelet transform has been applied to image processing and speech recognition with great success, there have been only a few applications in machinery diagnostics, for example, the work of McFadden et al. in the application of the wavelet

transform to fault detection in a gearbox [24, 27]. Damage in bearing elements is one of major problem in rotating machines that can be detected by the wavelet transform [28, 29]. Fault detection and identification in a helicopter gear-box was carried out by Lopez et al. [30].

It has been shown that, in the diagnosis of faults in reciprocating machines, the wavelet transform may be considered as a satisfactory technique for extracting the characteristics of vibration signals [31]. Zhongxing and Liangsheng [32] used the wavelet packet technique to analyse the vibration signals of a compressor. In another approach, Dalpiaz and Rivola [2, 33] applied the wavelet transform to the condition monitoring and diagnostics of cam mechanisms. We note that in most of the above applications the Gaussian wavelet function was chosen as a mother wavelet function.

3.1. Software for Wavelets Transforms

A user-friendly software has been developed to permit the use of different methods of time-frequency analysis such as the Short-Time Fourier Transform, the Wigner-Ville Distributions, and the Wavelet Transforms. The program allows the user to carry out different distributions of Cohen's class of time-frequency methods such as the Choi-Williams Distribution and the Born-Jordan-Cohen Distribution. In addition, it provides different kinds of wavelet transforms, for example: the wavelet transform, the wavelet packet transform, and the wavelet transform by the Gabor Dictionary. In addition, the new technique of the "zoom in wavelet transform" makes it possible to obtain very satisfactory frequency resolution. This program has been developed especially for the diagnosis of defects in machinery, and includes most of the commonly-used methods of time-frequency analysis. We have tried to use those kernels and filters which are compatible with the current signals in machine diagnostics. The program has some interesting

options which are of considerable practical value in such cases. For example, de-noising by wavelet transform, which is an important tool in the analysis of noisy signals, allows the user to obtain an improved time-frequency representation.

Some examples from simulated signals have been used to verify the function and accuracy of the program. The first example is the sum of three sines: 300Hz, 1000 Hz and 3000 Hz; the time frequency plane shows three constant frequency bands. Although the wavelet transform of the signal, as shown in Figure 12(b), indicates a concentration of the signal's energy in the three bands, there is also the dispersion of this energy in the adjacent bands especially when an incorrect filter is chosen, as shown in Figure 12(c). On the other hand, it is impossible to determine the exact values of the frequencies by the logarithmic scale of the frequency axis.

The wavelet packet transform of this example gives better representation in the time-frequency plane than the wavelet transform of this signal (Figure 13). The linear scale of the frequency axis gives better frequency resolution. Filter selection plays an important role here also.

The matching pursuit algorithm gives the best representation of this signal, as shown in Figure 14. The resolution of frequencies in the time-frequency plane is very satisfactory.

The second example is a Dirac function in 0.1 sec. This function is an example of transitory signals. The wavelet transform of the example is shown in Figure 15. This time, the wavelet transform gives the best representation of the signal in the time-frequency plane. The peak appears exactly at 0.1 sec. The very good time resolution provided by the wavelet transform in the higher frequencies makes it a powerful tool for the detection of transitory phenomena in the signals.

The wavelet packet transform shows the Dirac function in approximately 0.1 sec (Figure 16). Its time

resolution is not as satisfactory as that of the wavelet transform. There is a difference between the results obtained by the wavelet transform and those obtained by the wavelet packet transform (the wavelet packet transform has better frequency resolution in the higher frequencies than the wavelet transform, but at the expense of a loss of time resolution in these frequencies).

The matching pursuit algorithm gives a representation of the signal that is not as good as that given by the wavelet transform, but is better than that given by the wavelet packet transform, as shown in Figure 17.

The next example is an amplitude-modulated cosine at 1000 Hz. The wavelet transform representation of the signal in the time-frequency plane shows the modulation of the signal. To obtain a clear representation of this signal, it is preferable to see simultaneously the mean-square wavelet map (three-dimensional representation) of the signal, as shown in Figure 18. The wavelet packet transform of the signal accompanied with the mean-square wavelet packet map of the signal show in Figure 19. Here, we use Haar wavelet function which provides a good time resolution. To obtain more clear representation of the signal in frequency, we can use a Daubechies 20 wavelet function which provides good frequency resolution at the expense of a loss of time resolution.

For this type of signal, the matching pursuit algorithm is not recommended because the modulation is not displayed (Figure 20).

The final example is a frequency-modulated signal at 1000 Hz. The wavelet transform and the mean-square wavelet map of the signal are shown in Figure 21. In the time-frequency plane, the representation of the signal is once again unclear. If there are other components in the signal, it will be very difficult to identify the signal. The mean-square wavelet map of the signal is not clear, either.

The wavelet packet transform gives a better representation of the signal than the wavelet transform; in

particular, the mean-square wavelet packet map of the signal is clear, as shown in Figure 22.

Again, the matching pursuit algorithm cannot be recommended because the frequency modulation cannot be identified (Figure 23).

3.2. Experimental application of the wavelet transforms

After comparing the theoretical behavior of several variations of the wavelet transform when applied to different signals, we now investigate signals obtained from experimental cases. A pin-point defect with known characteristics and location was created on a rolling bearing. The test set-up consisted of an electric motor, a shaft mounted on two journal bearings (SKF 1210 EKTN9 self-aligning, double row), labelled A and B, a gear-box and a break to impose the load. The defect was created on support A by scratching the inner raceway of the bearing with an electric pen. Figure 24 shows the experimental set-up.

The vibration signal was measured on support A by an accelerometer and transferred to an analyser. The measured signal was converted into American National Standard Code for Information Interchange (ASCII) format and transferred to the in-house software program for analysis.

The frequencies of different types of bearing defect may be computed using the geometric characteristics of the bearing and the rotating frequency [34]. The geometric characteristics of the damaged bearing are as follows:

Pitch diameter $D=69$ mm

Diameter of the rolling body $d=10.32$ mm

Contact angle $\alpha = 7.87$ deg

Number of rolling elements $N = 17$ (per row)

Bearing frequency of rotation $F_r = 12.2$ Hz

The frequency defect caused by damage on the inner raceway of this bearing can be computed by the following formula:

$$F_i = \frac{F_r N}{2} \left[1 + \frac{d}{D} \cos(\alpha) \right] \quad (27)$$

Equation (25) gives us a value for the pass frequency on a point of the inner raceway which equals approximately 238 Hz. Note that the frequency of this type of defect has a special characteristic. The default frequency should be an amplitude-modulated wave at approximately 238 Hz with the frequency of modulation equal to the rotating frequency.

Figures 25-26 show respectively the wavelet transform and the wavelet packet transform of the vibrational signal of the defected bearing it is almost impossible to identify the defect by these figures because the original signal is very noisy. To obtain more clear representation of the signal, it is necessary to remove at first the noise from the signal. To do this, there are two possibilities in the software: De-noising by classical wavelet transform and De-noising by Matching Pursuit algorithm. Here, we use the de-noising by matching pursuit algorithm and The de-noised signal is called *dn-bearing*. Figures 27-28 show respectively the wavelet transform and the wavelet packet transform of the de-noised signal. As shown, the wavelet transform of the de-noised signal is clearly shown the repetitive peaks in frequency band 200–400 Hz. The frequency of amplitude modulation in this band is approximately 12.2 Hz which equals to the rotating frequency. Then, the defect in bearing may be easily be identified by the wavelet transform of the de-noised signal. The wavelet packet transform of this signal provides more frequency resolution but it is not

as clear as the wavelet transform of the signal. The default frequency is situated in frequency band 200-300 Hz.

3.3. Industrial application of the wavelet transform

In the last section, the performance of wavelet transforms for a defect created on the inner raceway of a bearing was described. In this section, the efficiency of wavelet transforms for an industrial case without any prediction of defects is demonstrated. This case comes from the defective gear-train of a hoist drum in a large shovel operating at an open-pit iron mine.

Gearbox faults may be classified into shaft (misalignment, imbalance) and tooth (wear, scuffing, cracking) related problems. Damage to a single tooth is called a local tooth fault, and will be investigated in this section. Vibration signals measured on a gearbox include the tooth-meshing frequency, transient events caused by defects, gearbox resonance vibrations and system and sensor transmission characteristics. These vibration signals are non-stationary signals which require specific techniques because application of the conventional methods, such as Fourier analysis, to gearbox fault detection are often difficult. Time-frequency methods provide new techniques for the analysis of non-stationary signals and have advanced capabilities for the separation of different phenomena. The application of some time-frequency methods to the analysis of gearbox faults has been described in [3, 4], and here, the application of another group of time-frequency methods, called time-scale analysis, is presented.

The time signal of the damaged gearbox and its wavelet transform are shown in Figure 29. The repetitive pulses in the wavelet transform in the band between 320 Hz and 640 Hz are caused by a broken tooth. The mean square wavelet map of this signal gives representation of the wavelet transform in three dimensions. The wavelet packet transform of the signal in Figure 30 gives not only a better time-frequency

representation of the signal but also better frequency resolution than the wavelet transform. The mean square wavelet packet of the signal clearly shows the pulses.

The time-frequency plane projection by the Gabor Dictionary of the signal is shown in Figure 31 but it is not easy to obtain the characteristics of the signal from this figure.

Although the mean square wavelet packet map of the signal gives the best representation of the signal, the frequency resolution of the signal may not be as fine as is needed. To obtain a finer frequency resolution, we can use the zoom in wavelet transform which is based on choosing the best trees in the filter bank. By this method, first, the desired frequency band is selected and, second, a suitable frequency resolution is achieved by wavelet packet transform of this frequency band. A zoom in wavelet transform in the frequency band between 320 Hz and 640 Hz is shown in Figure 32.

4. CONCLUSION

The above study has shown the performance of a new method for the diagnosis of defects in machinery.

We have demonstrated that the wavelet transform provides a high frequency resolution in the lower frequencies and a high time resolution in the higher frequencies. This characteristic of the wavelet transform may be advantageous in machinery fault detection. The wavelet functions play an important role in obtaining a good representation of a signal and they are chosen in accordance with the characteristics of the signal.

The wavelet packet transform is a full tree filter bank which gives a linear-scale frequency axis. It gives better frequency resolution than the wavelet transform but the latter gives superior time resolution. In machine monitoring and fault detection, it is sometimes necessary to have high frequency resolution in order

to identify the type of defect and, in this case, one could recommend the use of the wavelet packet transform. However, this approach does result in a loss of information in the time domain and the time-frequency representation becomes complicated. For this reason, we have presented a new technique which is called the “zoom in wavelet transform”. This technique permits us to obtain desirable frequency resolution with clear time-frequency representation.

This article has also presented an easy-to-use software package which includes the majority of methods of time-frequency analysis and compares the wavelet transforms with other methods. The software is equipped with several interesting options such as a new method of de-noising by wavelet transform. This method, which has been applied recently in signal processing, improves the time-frequency representation of noisy signals.

The transient and the time-varying signals in machine condition monitoring present different behavior in their time-duration. The adaptive wavelet transforms are powerful tools which are capable of decomposing the signal into those waveforms that are best adapted to the signal structure.

A computer program implementing the wavelet transforms has been used to compare the performance of different wavelet methods. It has been shown, by the numerically generated signals and two experimental tests on a damaged bearing and a broken gear tooth, that the wavelet analysis methods are effective in machine condition monitoring especially when a transient phenomenon exists in the signal. In the case where a defect in a machine generates amplitude-modulation signals or frequency-modulation signals, it is preferable to use other time-frequency methods such as the Wigner-Ville distributions or the STFT.

5. REFERENCES

1. P. Grivelet 1990 Proceedings of the IMMDC Congress, Los Angeles, 393-399, Monitoring of Reciprocating Compressors automatics Machines.
2. G. Dalpiza and A. Rivola 1995 2nd International Symposium Acoustical and Vibratory Surveillance Methods and Diagnostic Techniques, 327-338, Fault Detection and Diagnostics in Cam Mechanisms.
3. M. S. Safizadeh, A. A. Lakis and M. Thomas 1999 École Polytechnique de Montréal, Technical Report No. EPM/RT-99/05, Application of Short-Time Fourier Transform in Machine Fault Detection.
4. M. S. Safizadeh, A. A. Lakis and M. Thomas 1999 École Polytechnique de Montréal, Technical Report No. EPM/RT-99/06, Fault Detection and Identification using Wigner-Ville Distributions.
5. J. Morlet and Al 1982 Geophysics 47(2), 203, Wave Propagation and Sampling Theory-part II: Sampling Theory and Complex Waves.
6. A. Grossmann and J. Morlet 1984 SIAM J. Math. Anal. 15, 723-736, Decomposition of Hardy Functions into Square Integrable Wavelets of Constant Shap.
7. S. Mallat 1989 IEEE Transaction on Pattern Analysis and Machine Intelligence 11(7), 674-693, A theory for Multi resolution Signal Decomposition: The Wavelet Representation.
8. Y. Meyer 1990 Ondelettes et Opérateurs (two volumes), Paris: Hermann.
9. Y. Meyer 1992 Les Ondelettes Algorithmes et Applications, PP. 127-133, Paris: Armand Colin.
10. I. Daubechies 1988 Commun. Pure Appl. Math., Vol. XLI, 909-996, Orthonormal Based of Compactly Supported Wavelets.

11. I. Daubechies 1992 Ten Lectures on Wavelets, Philadelphia: SIAM.
12. ---- 1993 IEEE Trans. Signal Process. 41(8), 2591-2606, A Discrete-Time Multiresolution Theory.
13. M. Vetterli and J. Kovacevic 1995 Signal Processing in Wavelets and Subband Coding, Englewood Cliffs, NJ: Prentice-Hall.
14. N. Hess-Nielsen and M. V. Wickerhauser 1996 Proceedings of the IEEE 84(4), 523-539, Wavelets and Time-Frequency Analysis.
15. K. Ramchandran and M. Vetterli 1996 Proceeding of the IEEE 84(4), 541-560, Wavelets, Subband Coding and Best Bases.
16. O. Rioul and M. Vetterli 1991 IEEE SP Magazine, 14-38, Wavelet and Signal Processing.
17. S. Mallat 1987 Tech. Rep., Dep. Comput. Inform. Sci., Univ. Pennsylvania, Philadelphia, PA, Multi resolution Approximation and Wavelets.
18. M. Vetterli 1992 IEEE Trans. Signal Processing 40(9), 2207-2232, Wavelets and Filter Banks : Theory and Design.
19. M. J. Shensa 1992 IEEE Trans. Signal Processing 40(10), 2464-2482, The Discrete Wavelet Transform: Wedding The À Trous and Mallat Algorithms.
20. R. R. Coifman and M. V. Wickerhauser 1992 IEEE Trans. Inform. Theory, Special Issue on Wavelet Transforms and Multires. Signal Anal. 38(3), 713-718, Entropy-Based Algorithms for Best Basis Selection.
21. S. Mallat 1993 IEEE Trans. Signal Processing 41(12), 3397-3415, Matching Pursuits with Time-Frequency Dictionaries.

22. D. L. Donoho and I. M. Johnstone 1994 CRAS Paris, t. 319, Ser I, 1317-1322, Idea De-noising in an Orthonormal basis chosen from a library of bases.
23. D. L. Donoho 1995 IEEE Trans. On Inf. Theory, 41(3), 613-627, De-noising by Soft-thresholding.
24. W. J. Wang and P. D. McFadden 1993 American Society of Mechanical Engineers, Petroleum Division(Publication)PD Structural Dynamics and Vibrations Proceedings of the 16th Annual Energy - Sources Technology Conference and Exhibition 52, Application of the Wavelet Transform to Gearbox Vibration Analysis.
25. W. J. Staszewski and G. R. Tomlinson 1994 Mechanical Systems and Signal Processing 8, 289-307, Application of the Wavelet transform to fault detection in a Spur gear.
26. P. D. McFadden 1994 Proceedings of an International Conference on Condition Monitoring, Swansea UK, 172-183, Application of the Wavelet Transform to Early Detection of Gear Failure by Vibration Analysis.
27. W. J. Wang and P. D. McFadden 1995 Mechanical Systems and Signal Processing 9, 497-507, Application of Wavelets to Early Gear Damaged Detection.
28. C. J. Li and J. Ma 1992 Sensors and Signal Processing for Manufacturing, ASME Winter Annu. Meet., Bearing localized Defect Detection Through Wavelet Decomposition of Vibrations.
29. Mei Hongbin 1995 Proceedings of the International Conference on Structural Dynamics, Vibration, Noise and Control, 1334-1339, Application of Wavelet Analysis to Detection of Damages in Rolling Element Bearings.
30. J. E. Lopez, R. Tenney and J. Deckert 1994 Proc. IEEE-SP Int. Symp. on Time-Frequency and Time-Scale Analysis, 217-220, Fault Detection and Identification Using Real-Time Wavelet Feature Extraction.

31. P. Grivelet 1990 Proceedings of the IMMDC Congress, Los Angeles, Monitoring of Reciprocating Compressors by vibration.
32. G. Zhongxing and Q. Liangsheng 1994 British Journal of Non-Destructive Testing 36(1), 11-15, Vibrational Diagnosis of Machine Parts Using the Wavelet Packet Technique.
33. G. Dalpiaz and A. Rivola 1997 Mechanical Systems and Signal Processing 11, 53-73, Condition Monitoring and Diagnostics in Automatic Machines: Comparison of Vibration Analysis Techniques.
34. R. G. Smiley 1983 Sound and Vibration 17(9), Rotating Machinery: Monitoring and Fault Diagnosis.

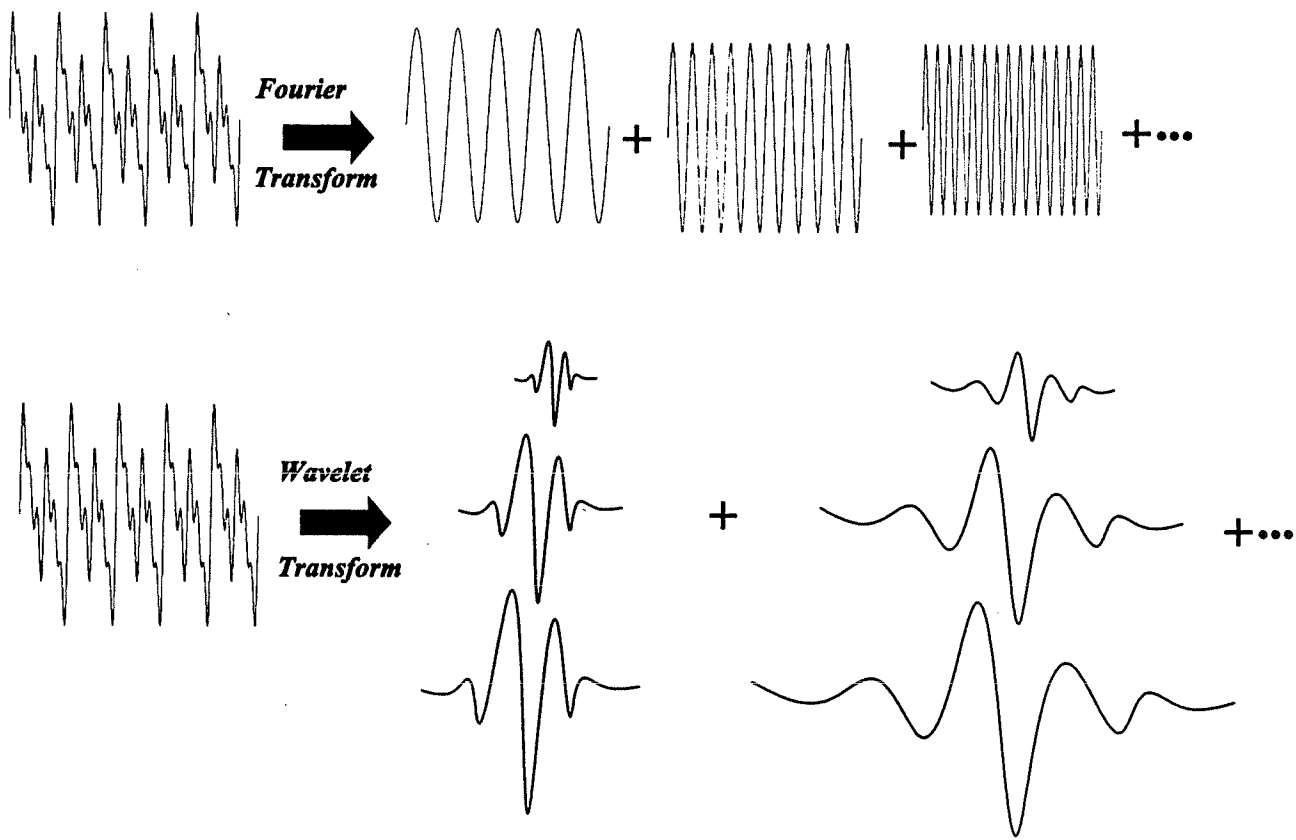


Figure 1: Comparison between Fourier transform and Wavelet transform.

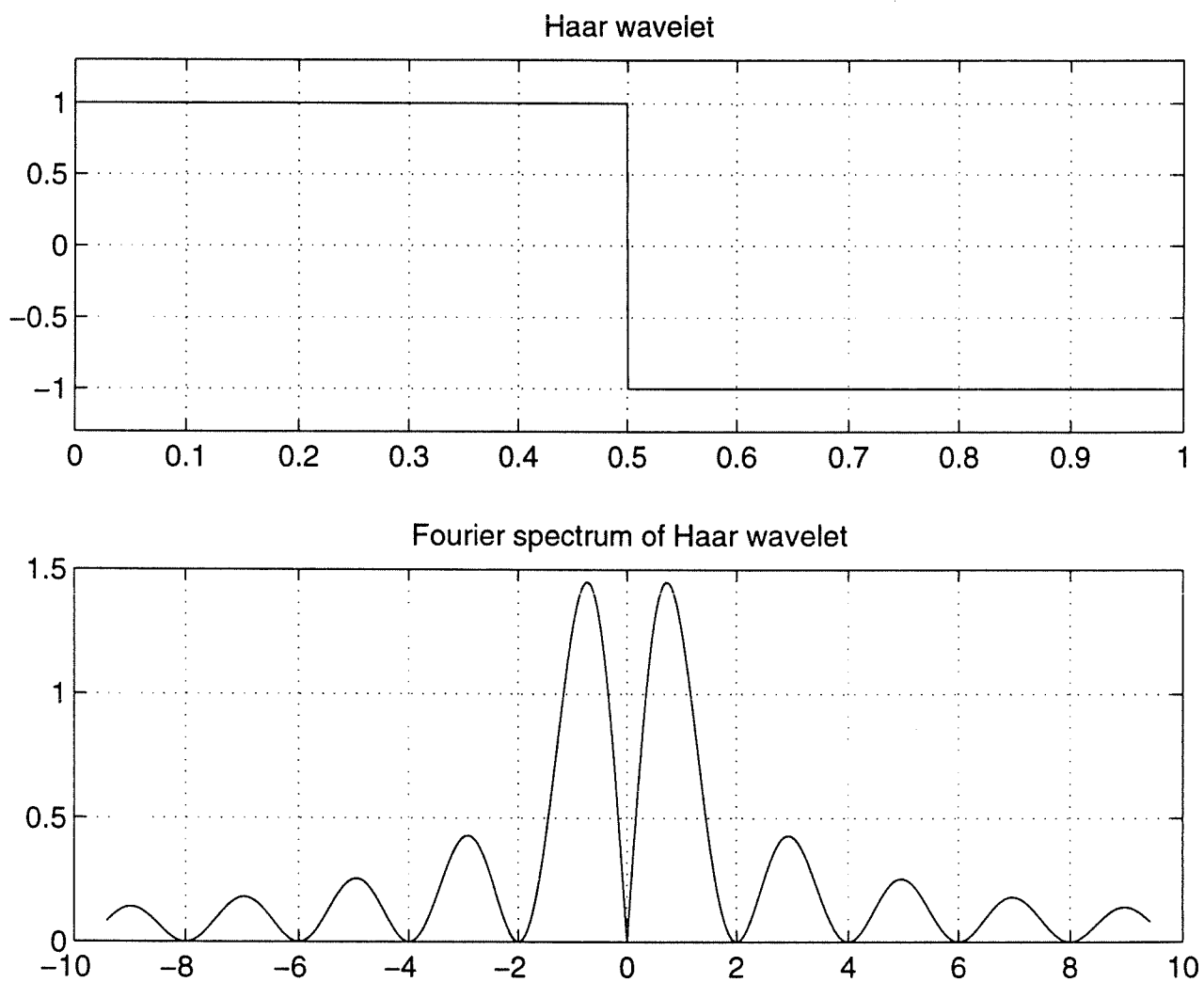


Figure 2: Haar wavelet and its Fourier spectrum.

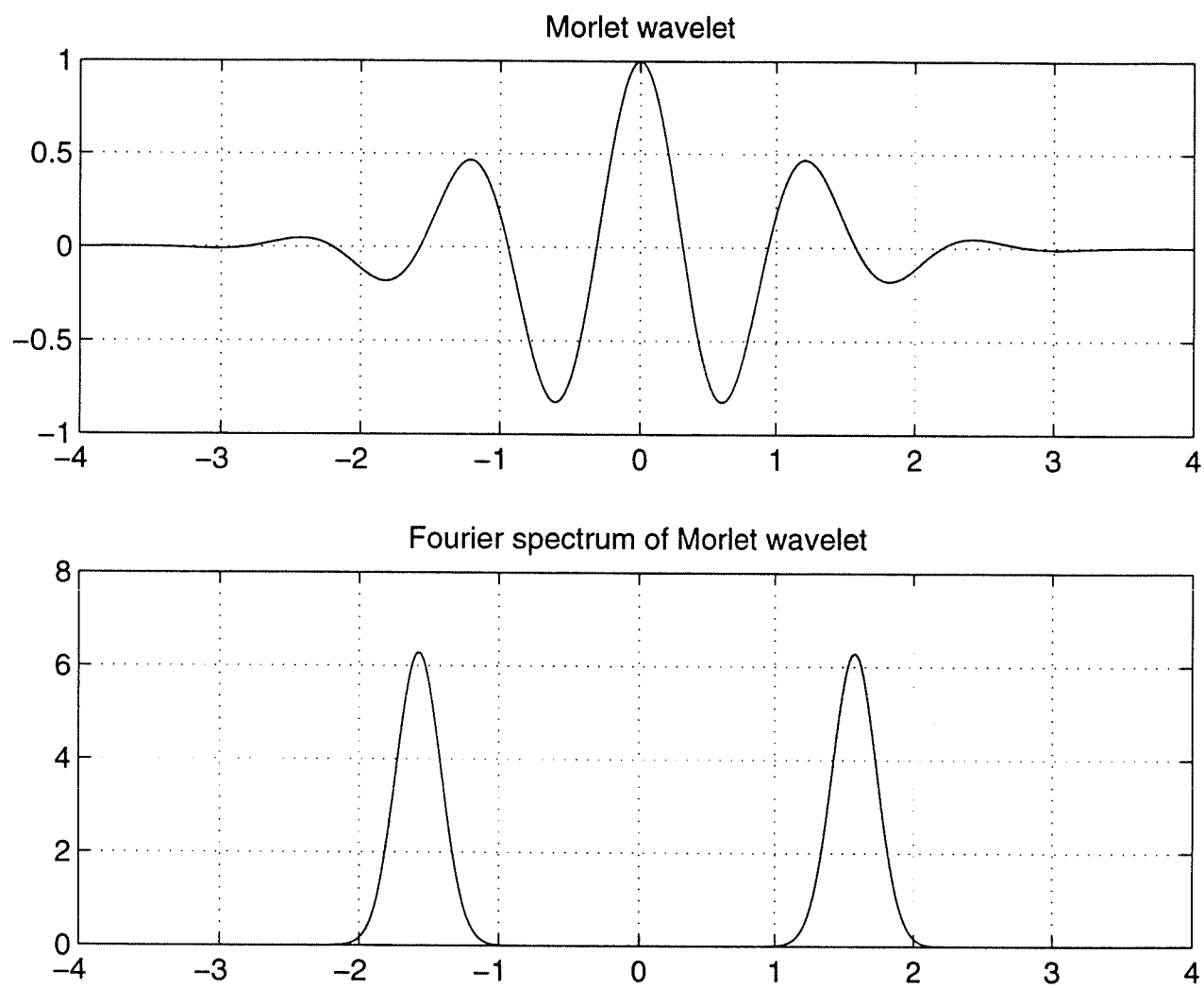


Figure 3: Morlet wavelet and its Fourier spectrum.

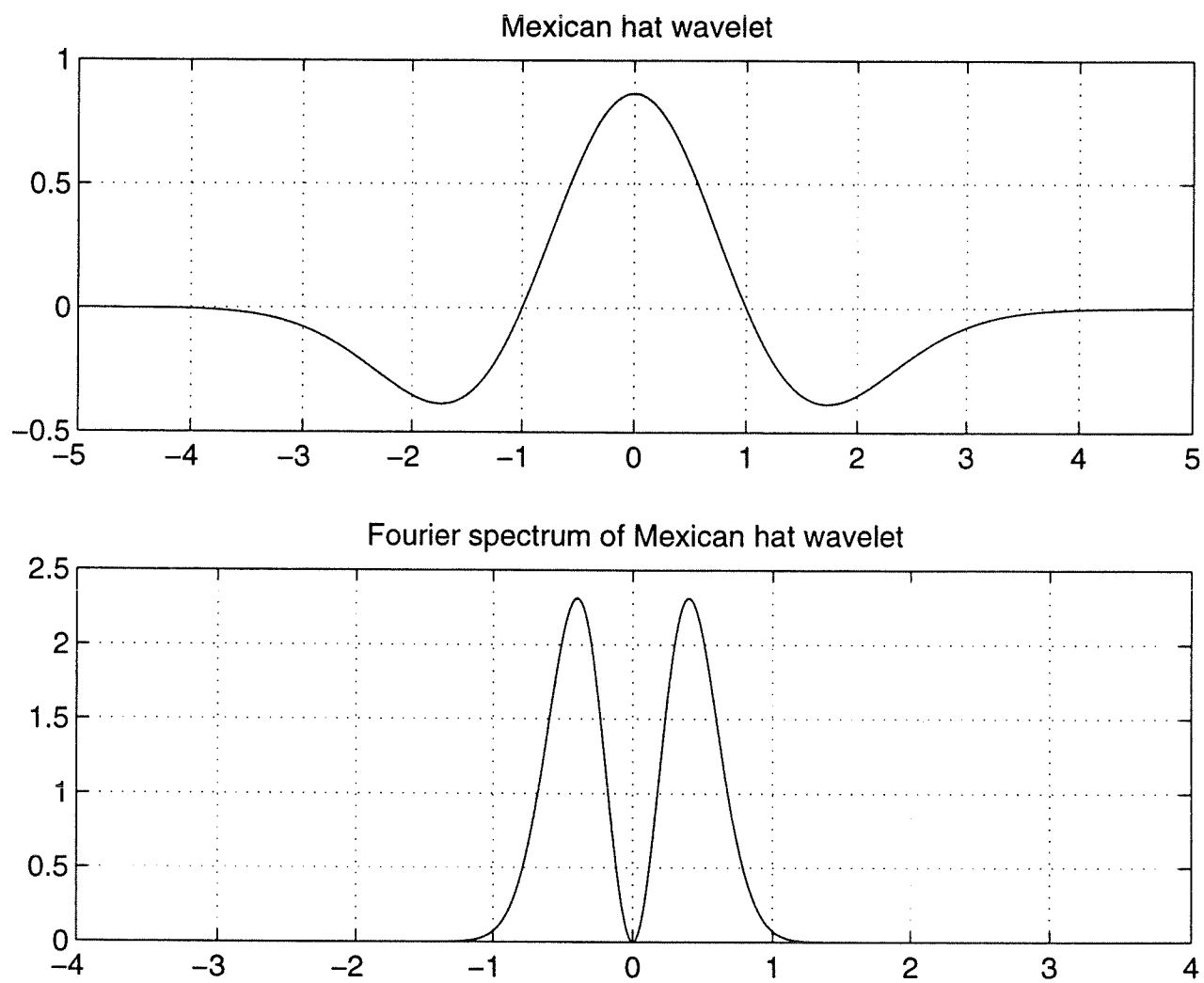


Figure 4: Mexican-hat wavelet and its Fourier spectrum.

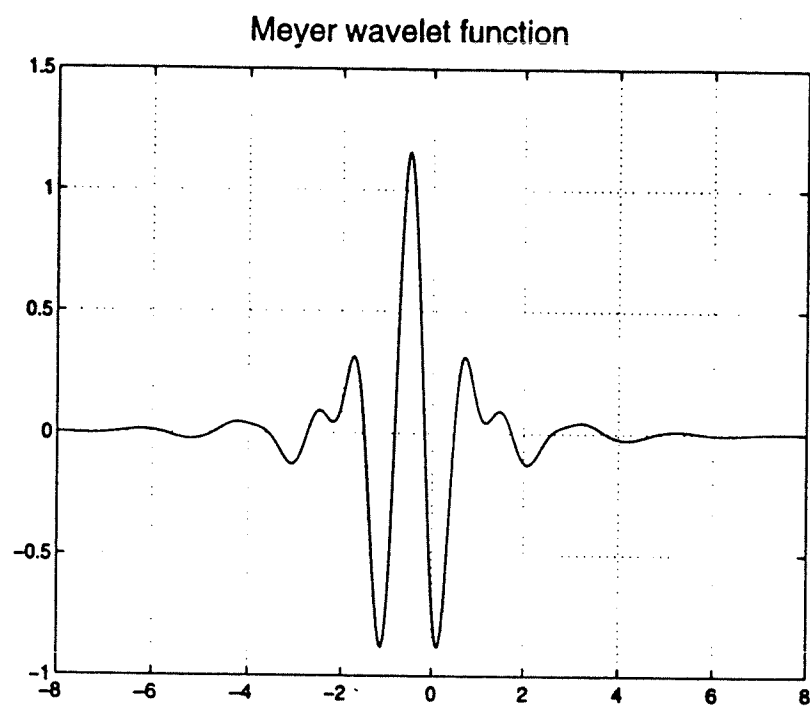


Figure 5: Meyer Wavelet function.

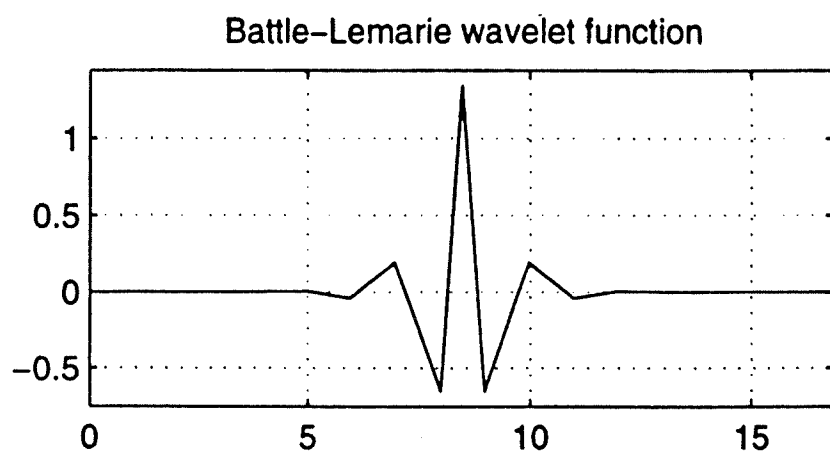


Figure 6: Lemarie-Battle wavelet function.

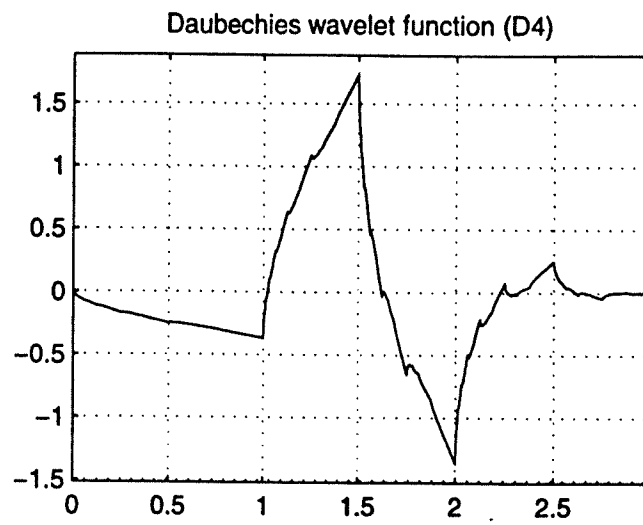
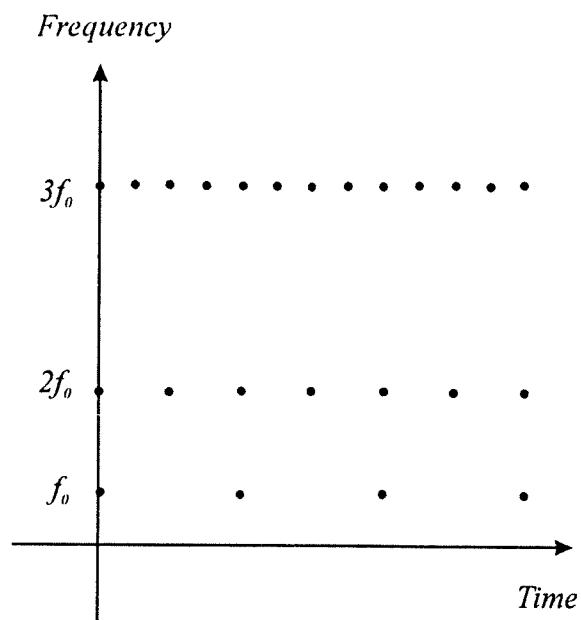
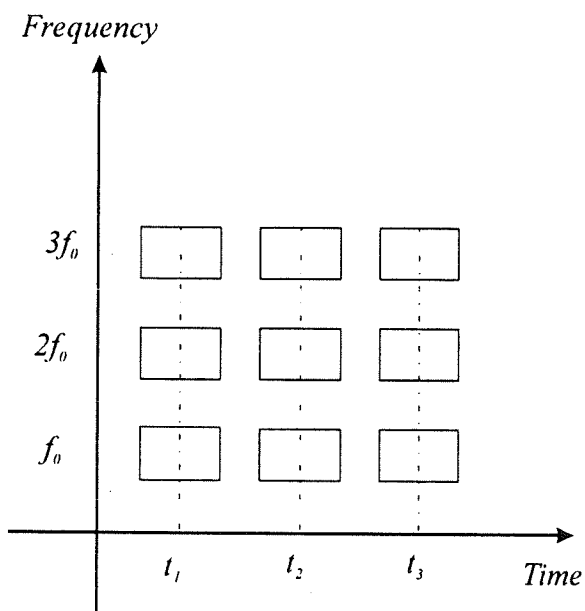


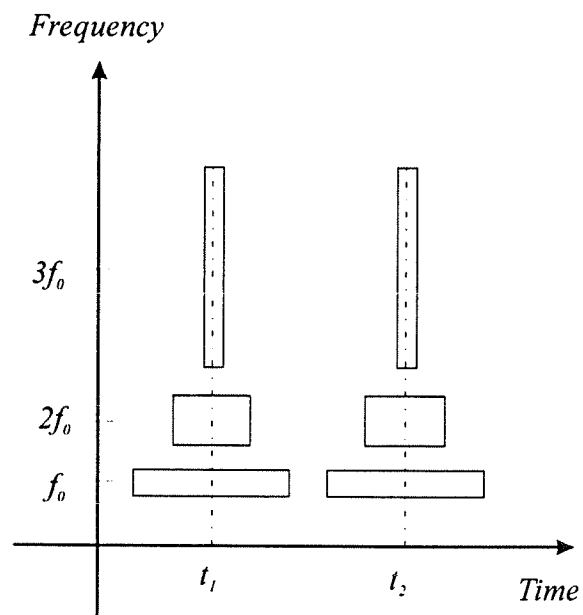
Figure 7: Daubechies wavelet function.



(a)

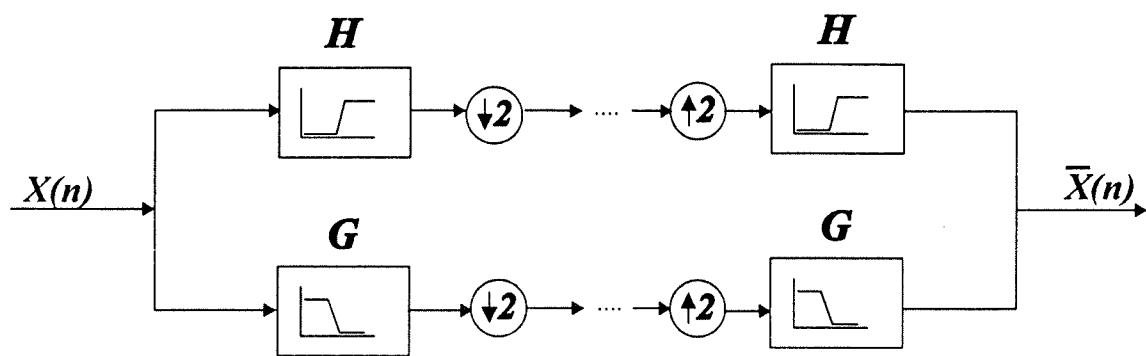


(b)

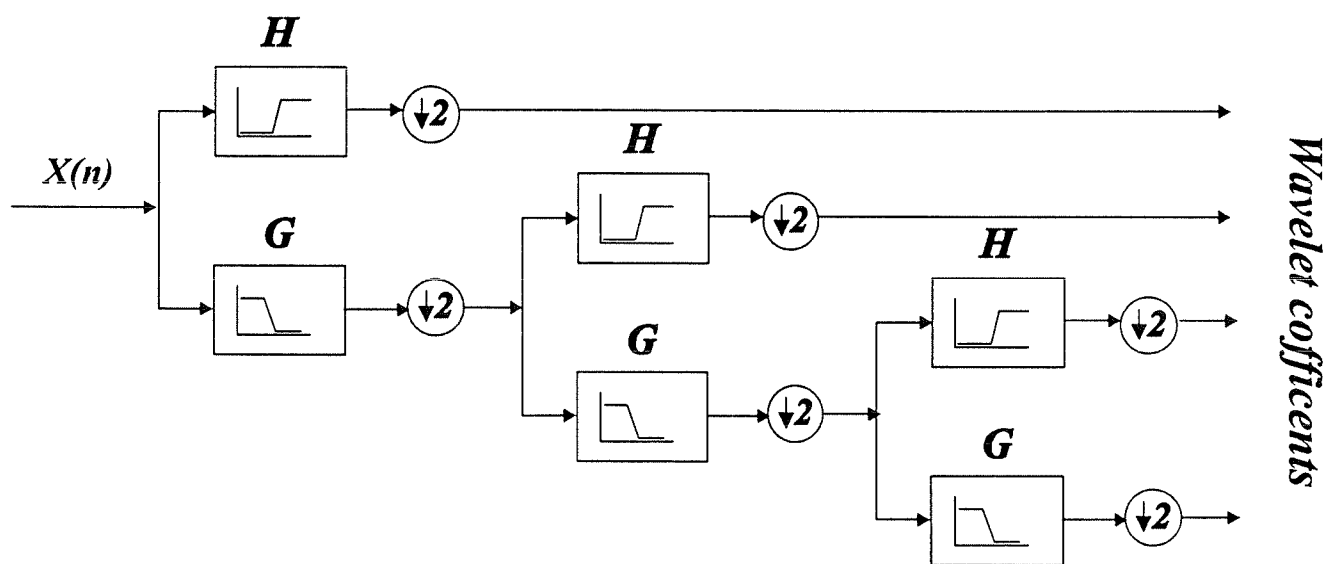


(c)

Figure 8: (a) Dyadic sampling grid in the time-scale plane
(b) Time-frequency plane of the Short-Time Fourier Transform
(c) Time-frequency plane of the wavelet transform



(a)



(b)

Figure 9: (a) Subband coding scheme H: high pass filter and G: low pass filter
(b) Filter bank tree of the discrete wavelet transform

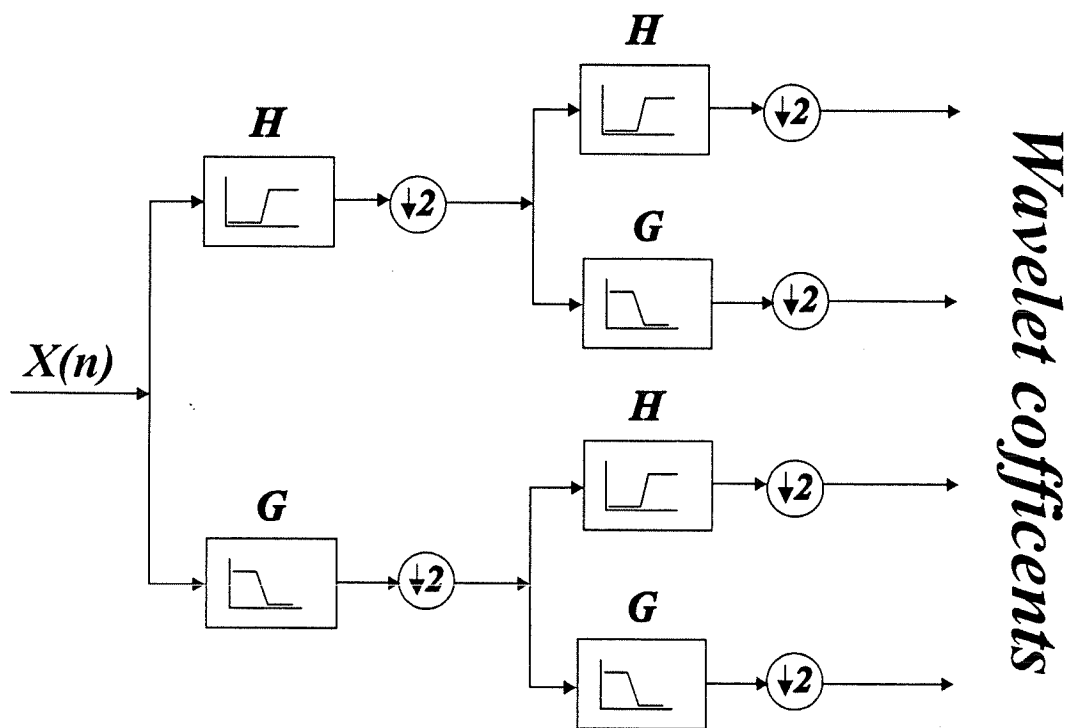


Figure 10: Filter bank tree of the wavelet packet transform.

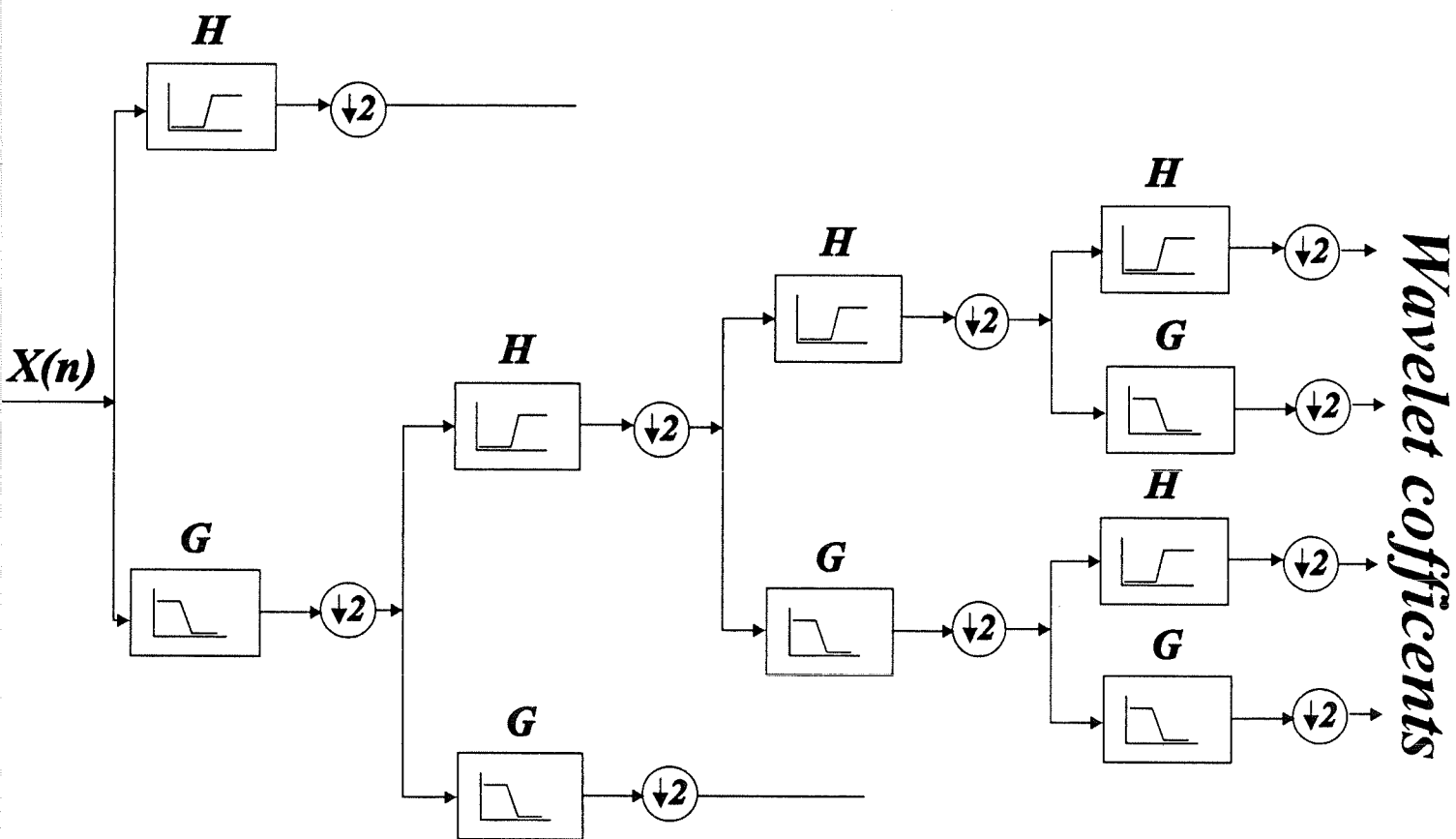


Figure 11: Block diagram of the “zoom in wavelet transform”.

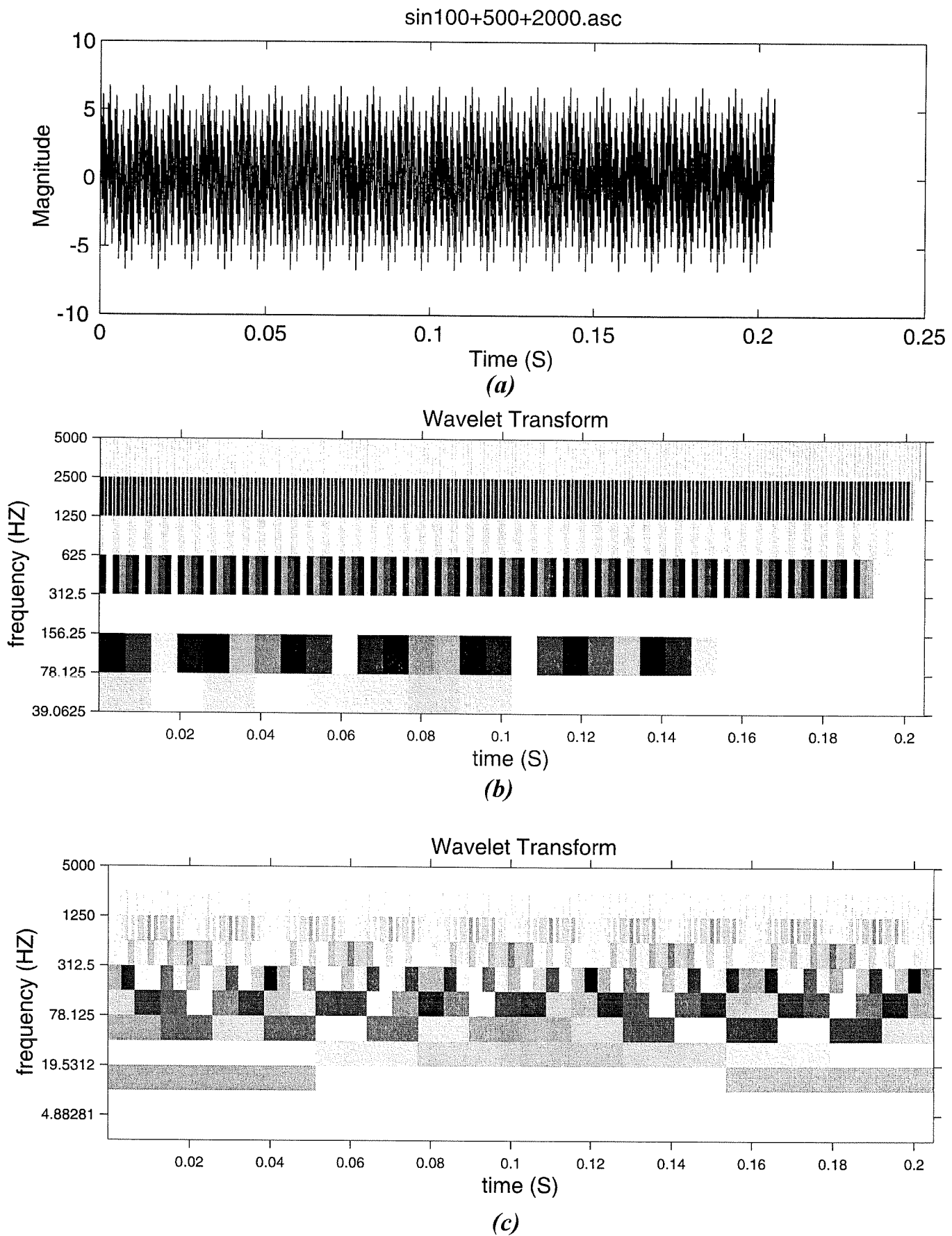


Figure 12: (a) Time representation of the sum of sine waves
 (b) The wavelet transform of the sum of sine waves by Daubechies filter (D20)
 (c) The wavelet transform of the sum of sine waves by Daubechies filter (D2)

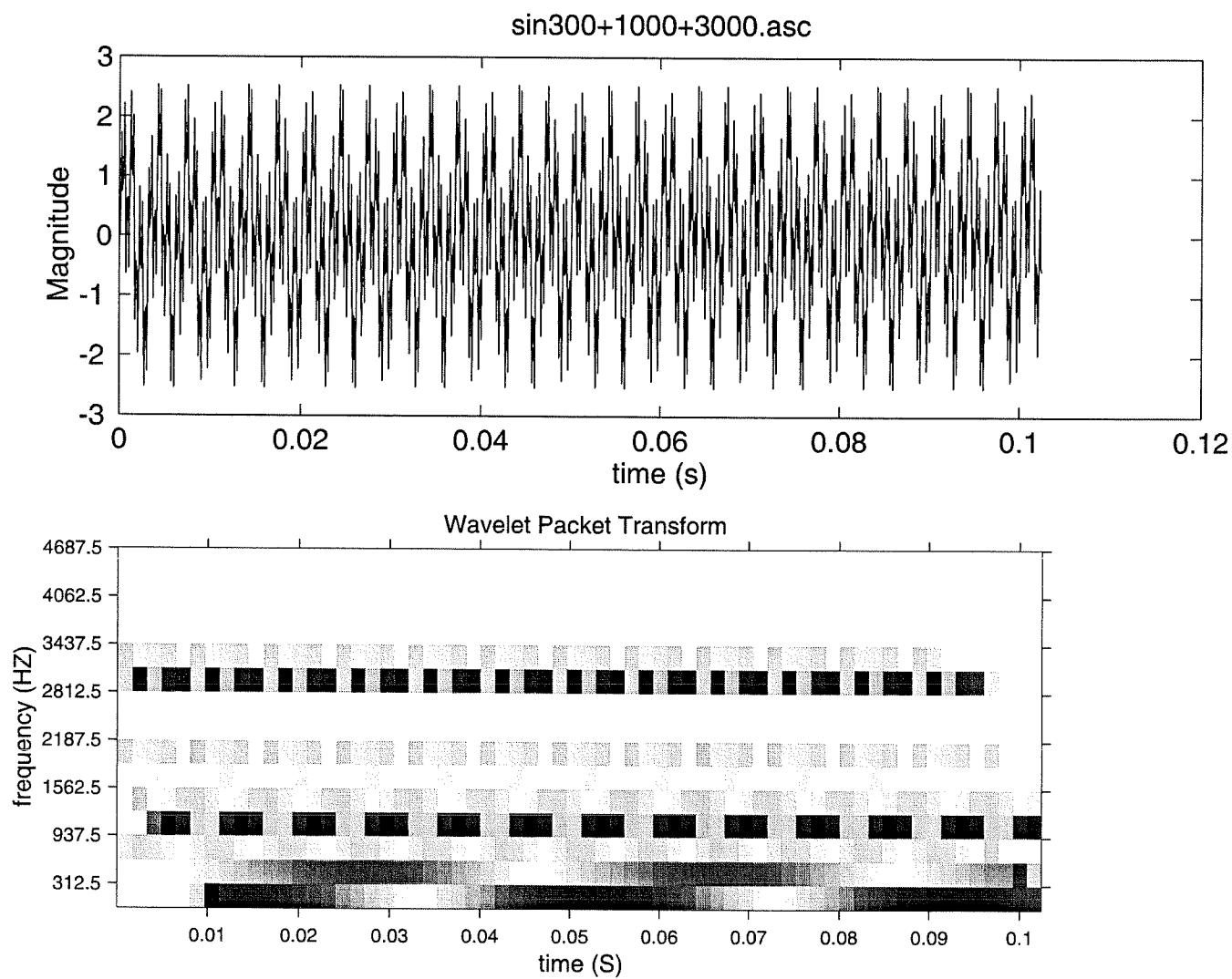


Figure 13: Wavelet packet transform of a sum of sines wave

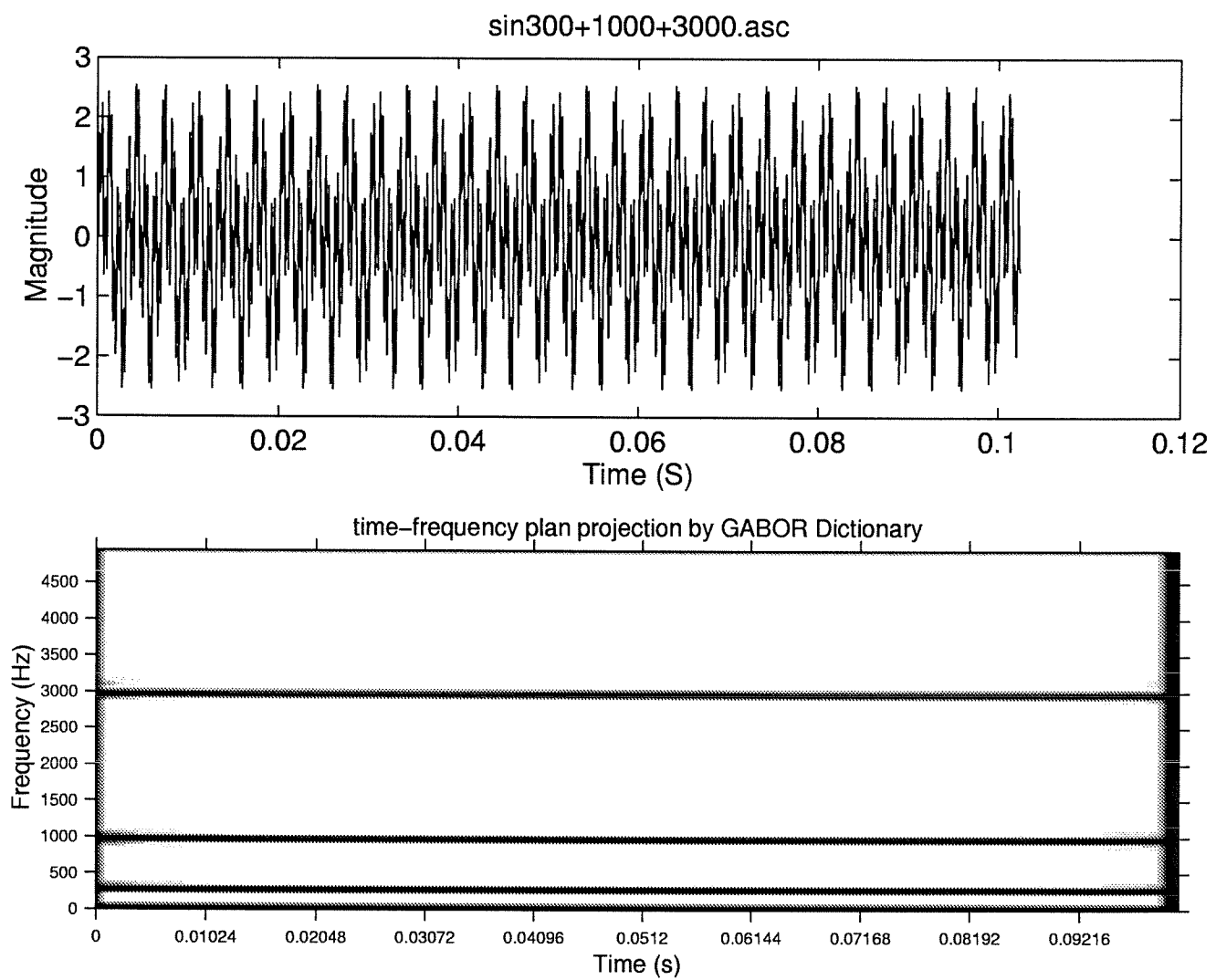


Figure 14: Time-frequency representation of a sum of sines wave by Gabor dictionary

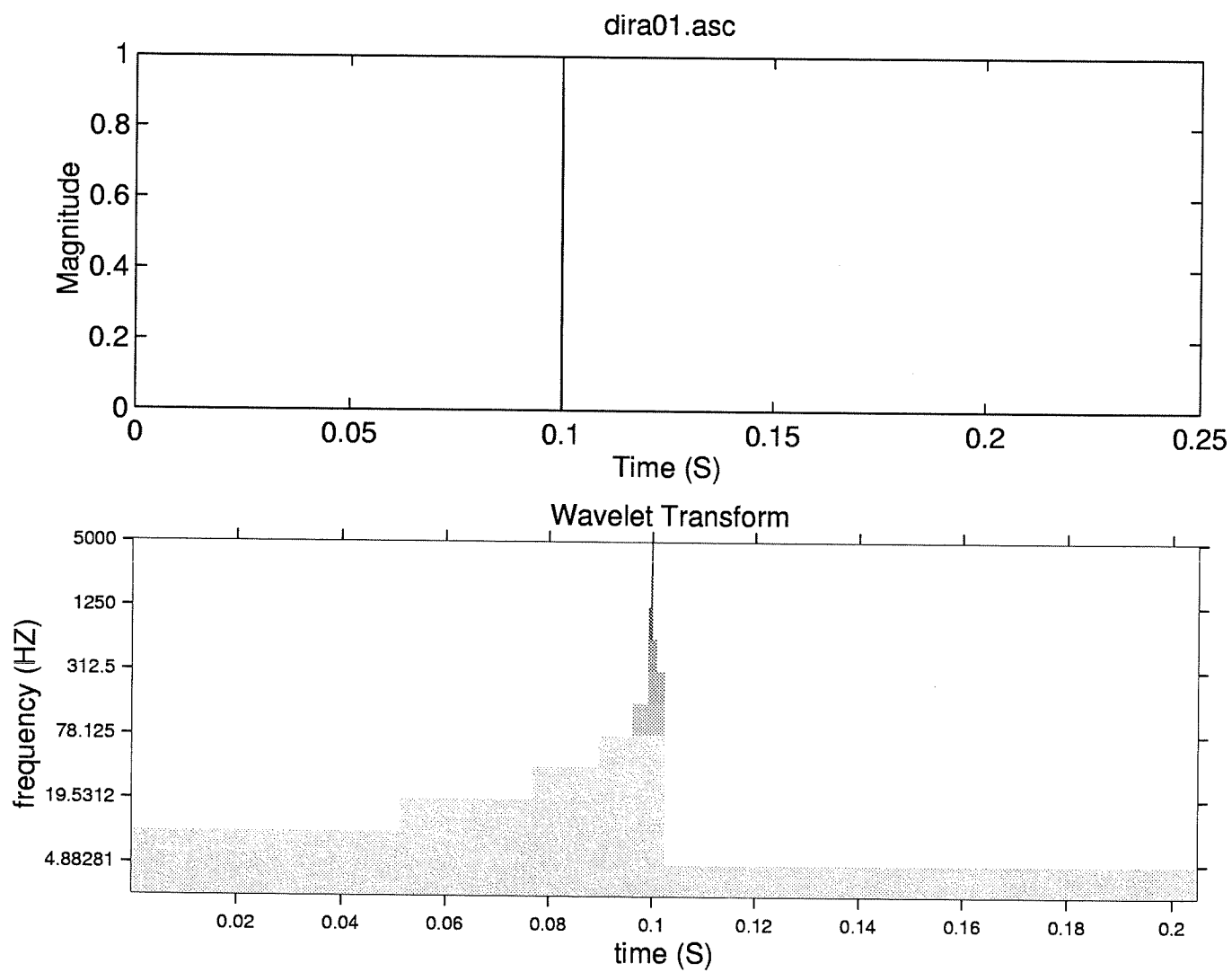


Figure 15: Wavelet transform of a Dirac function

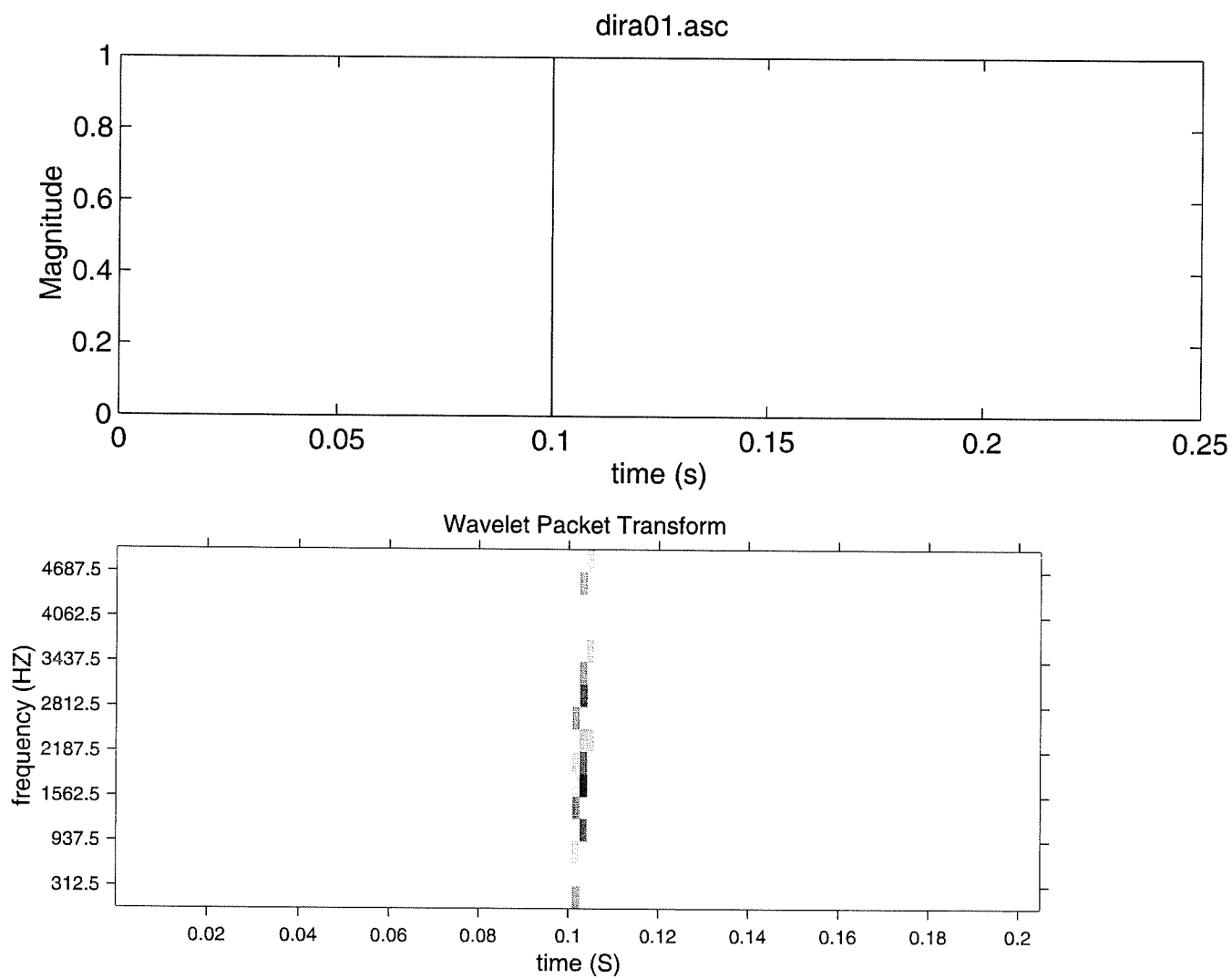


Figure 16: Wavelet packet transform of a Dirac function

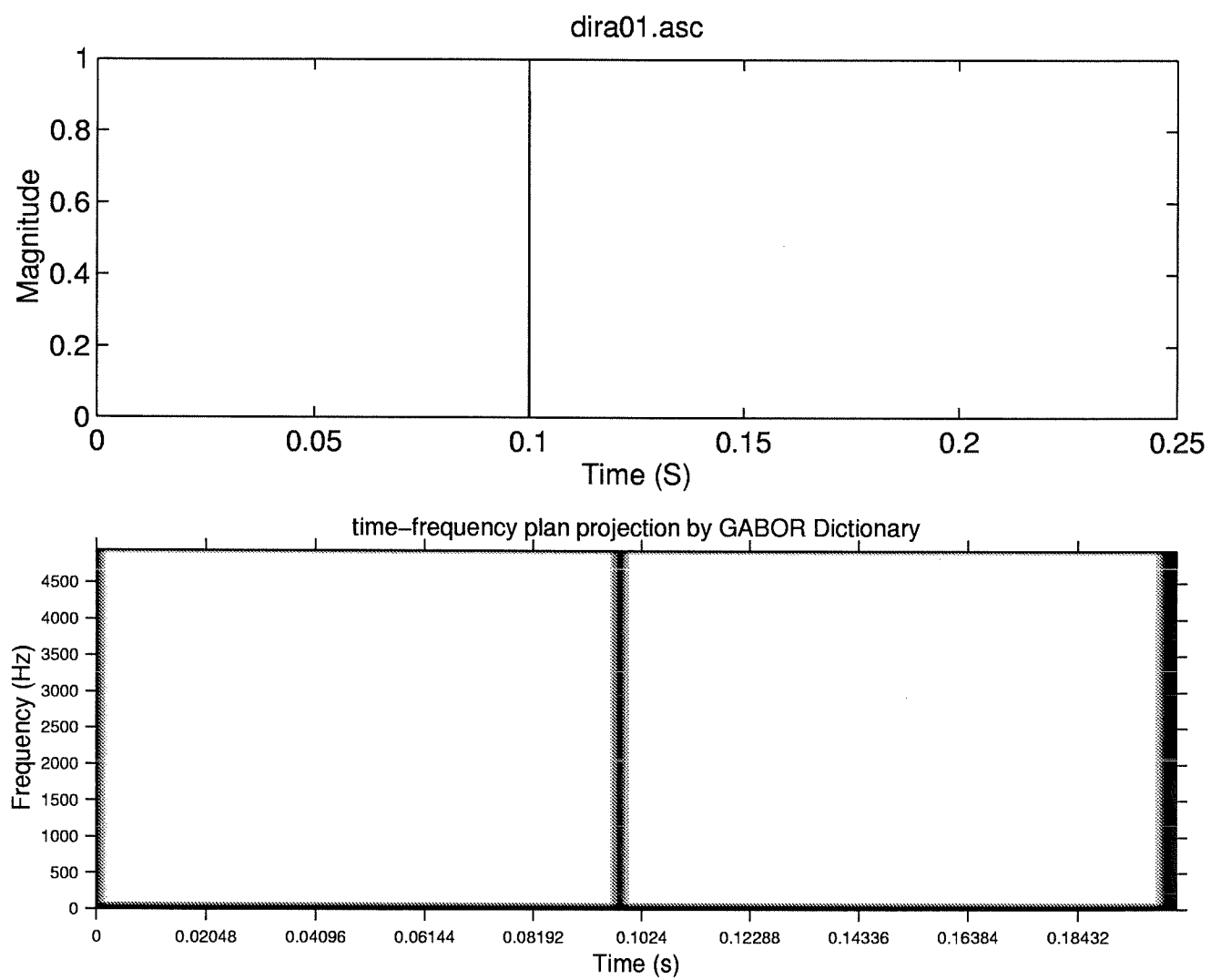


Figure 17: Time-frequency representation of a Dirac function by Gabor dictionary

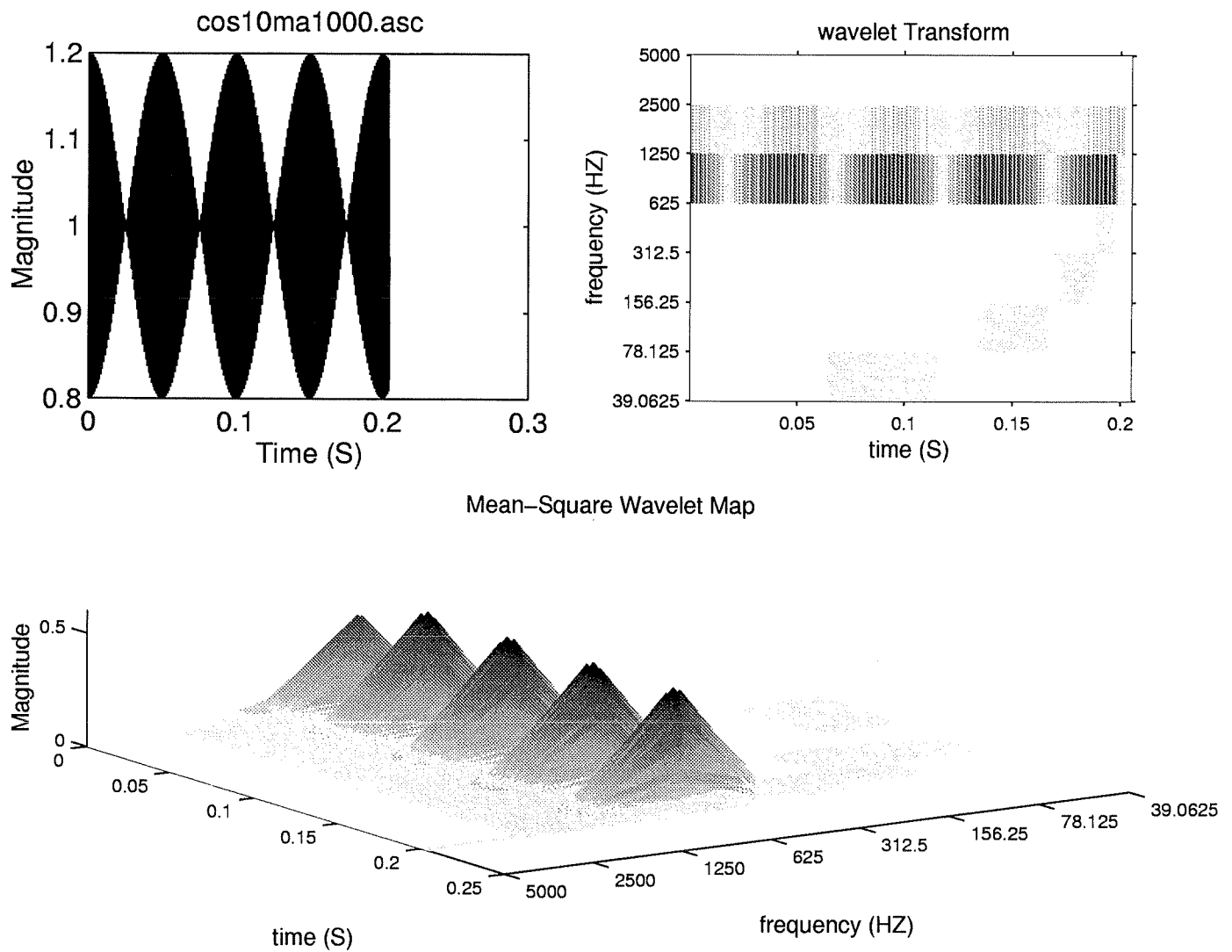


Figure 18: Wavelet transform and mean-square wavelet map of an amplitude-modulated sine

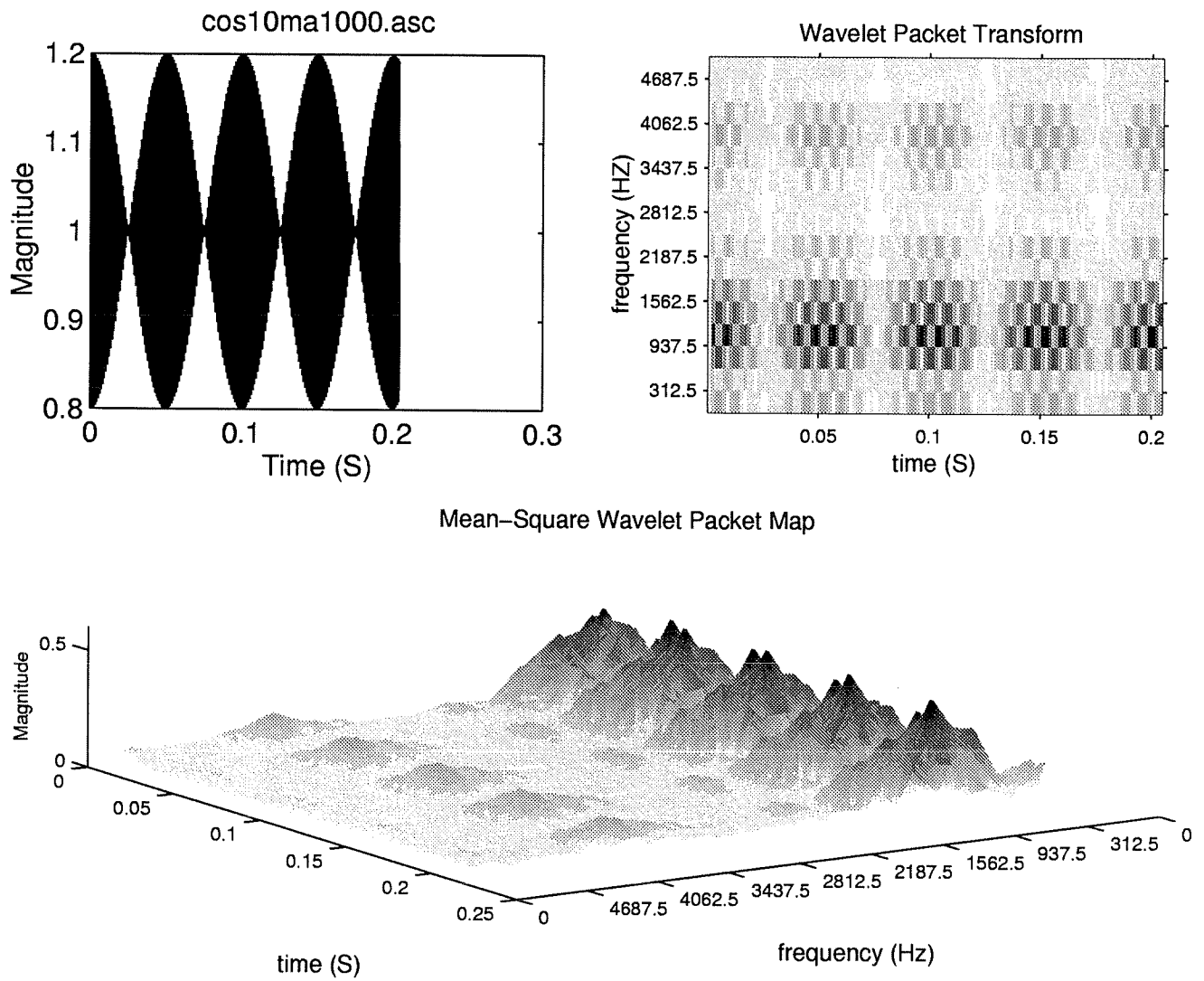


Figure 19: Wavelet packet transform and mean-square wavelet packet map of an amplitude-modulated sine

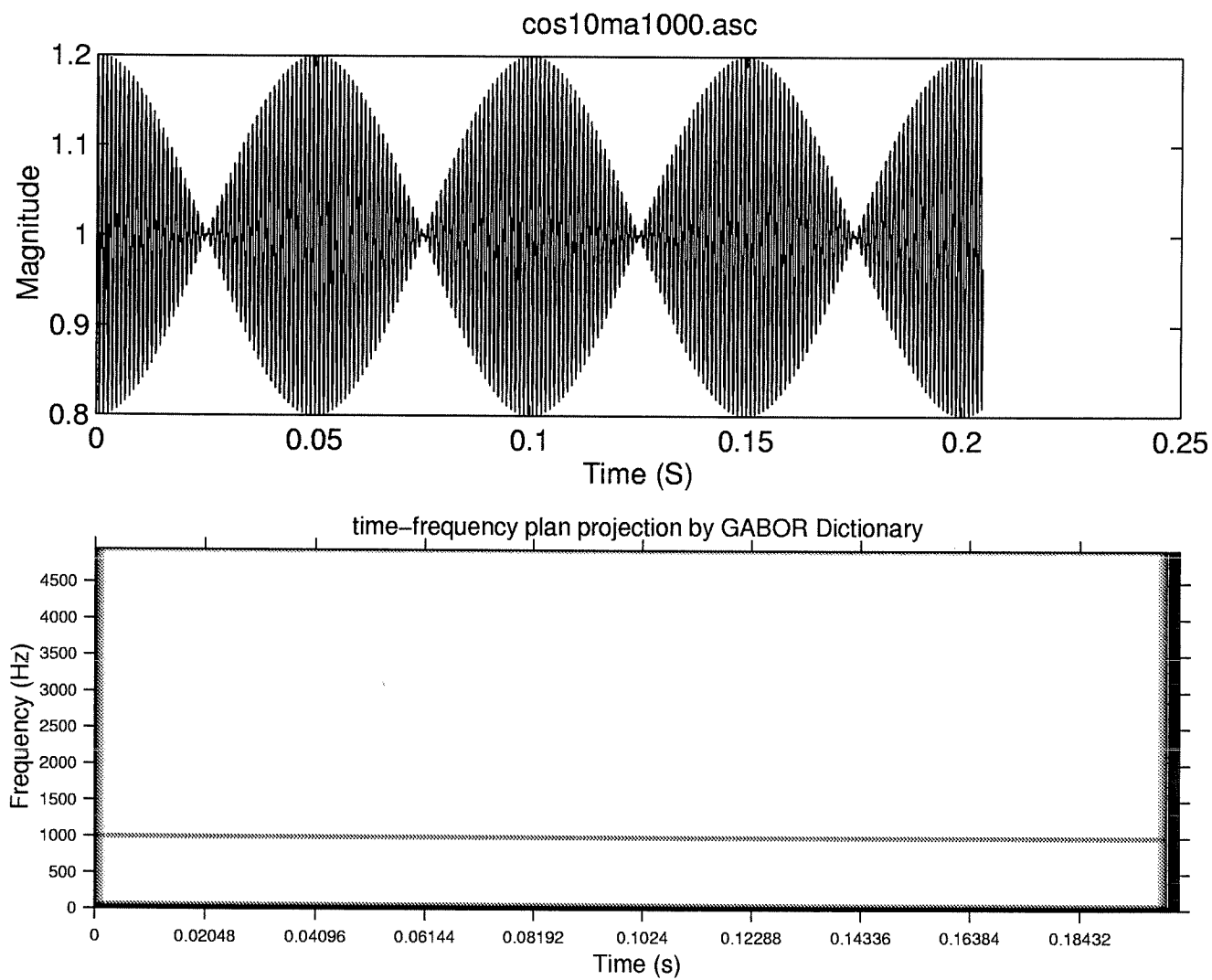


Figure 20: Time-frequency representation of an amplitude-modulated sine by Gabor dictionary

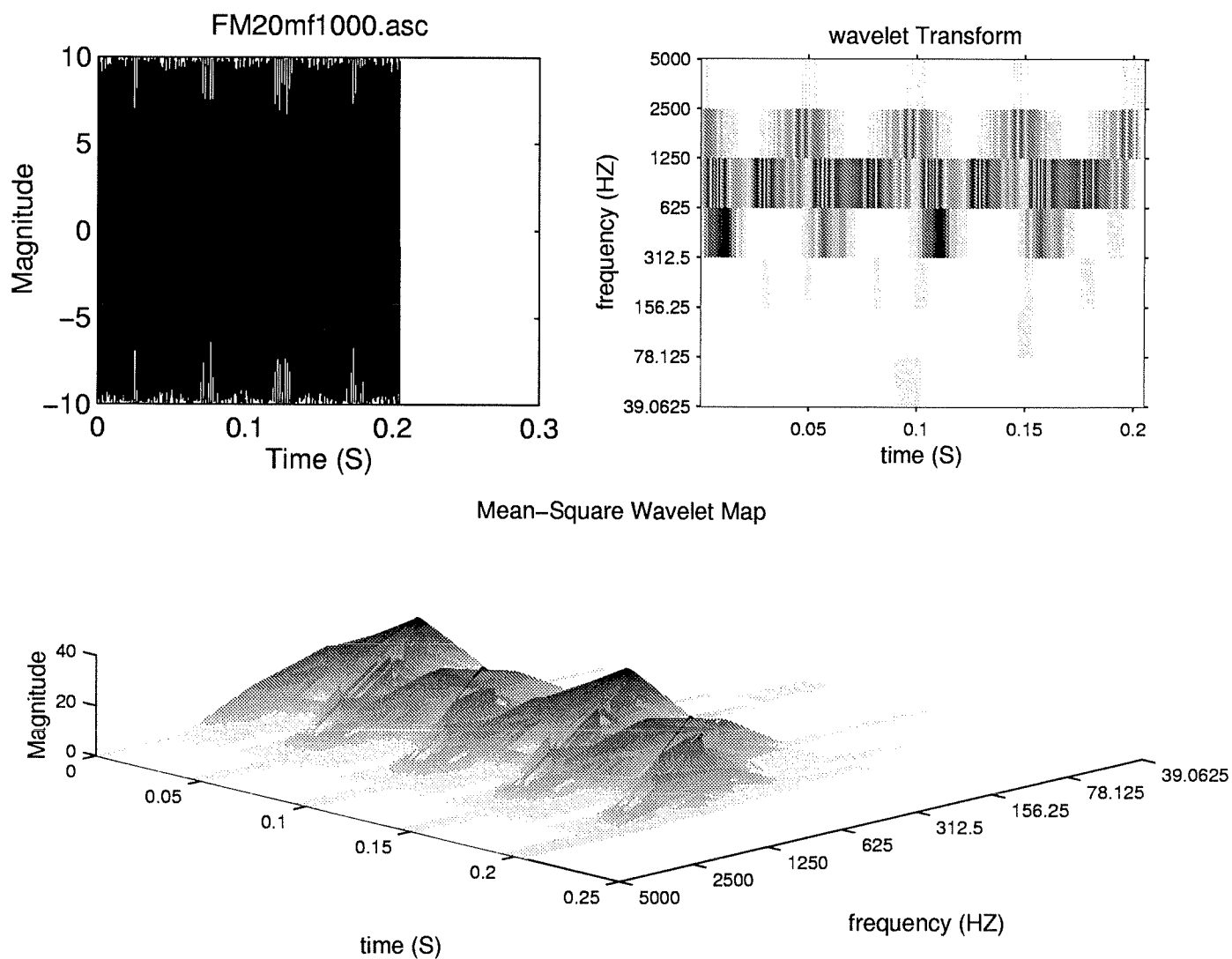


Figure 21: Wavelet transform and mean-square wavelet map of a frequency-modulated sine

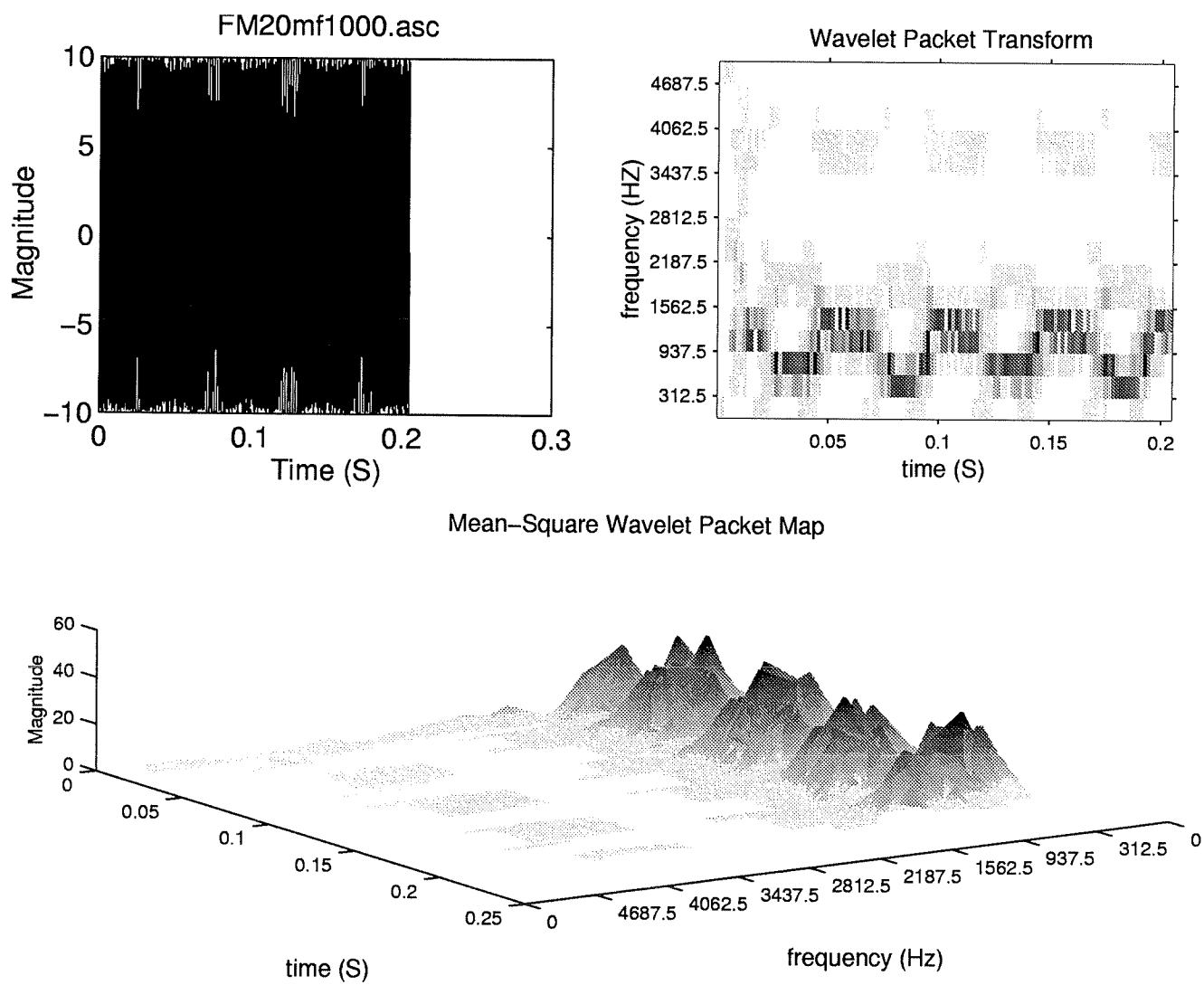


Figure 22: Wavelet packet transform and mean-square wavelet packet map of a frequency-modulated sine

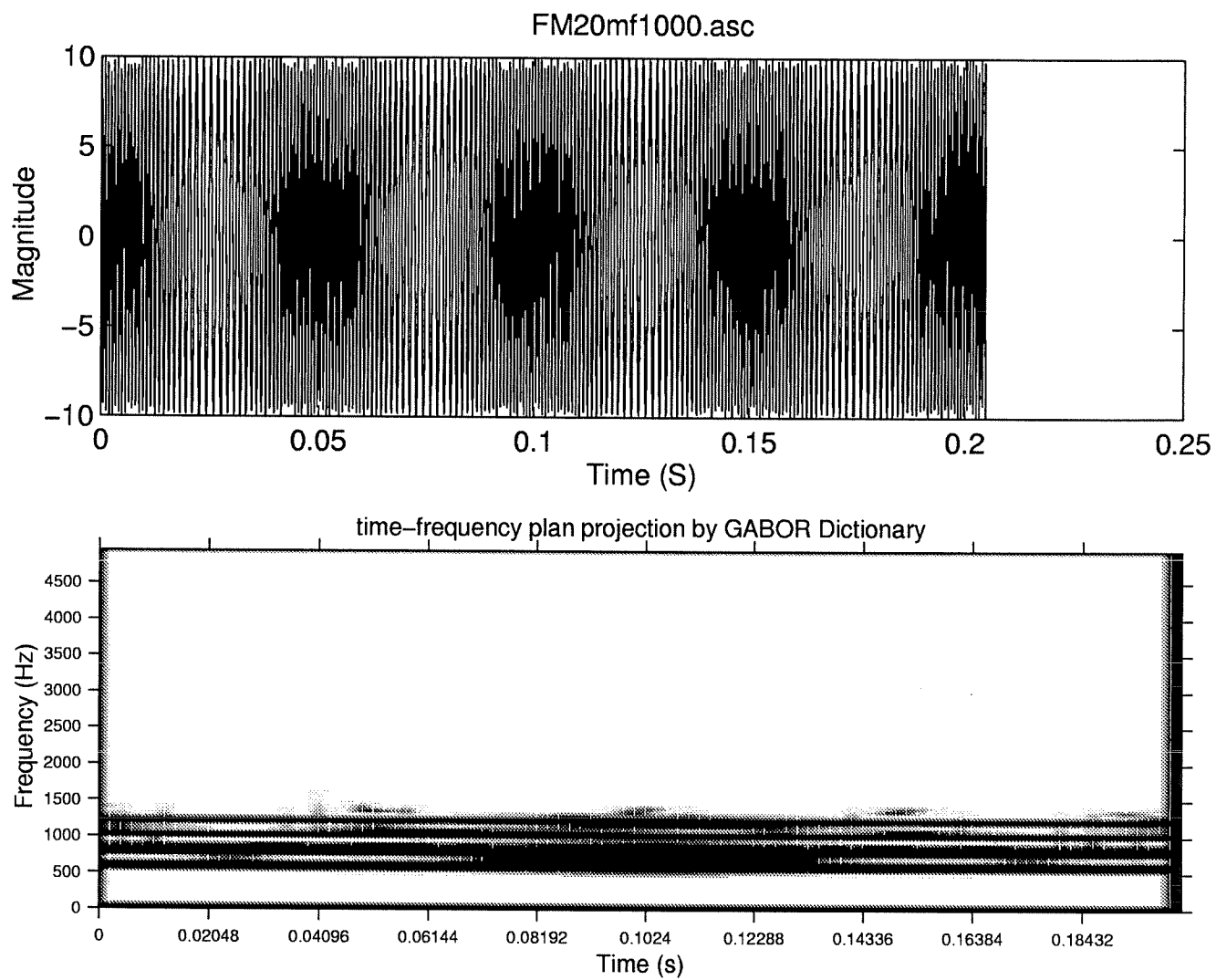


Figure 23: Time-frequency representation of a frequency-modulated sine by Gabor dictionary

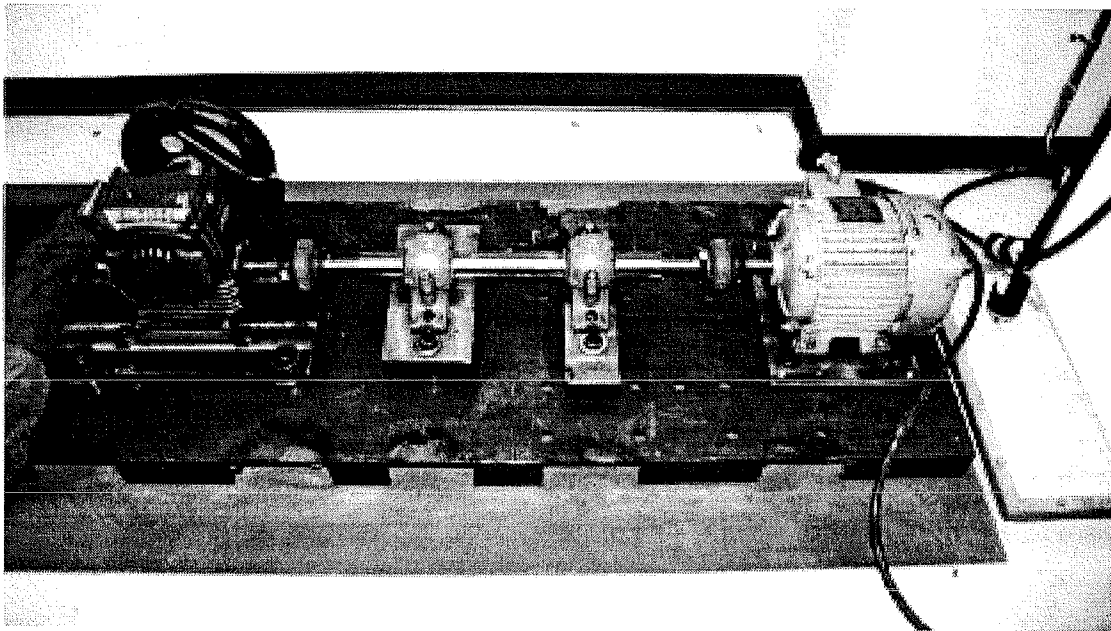


Figure 24: Test setup.

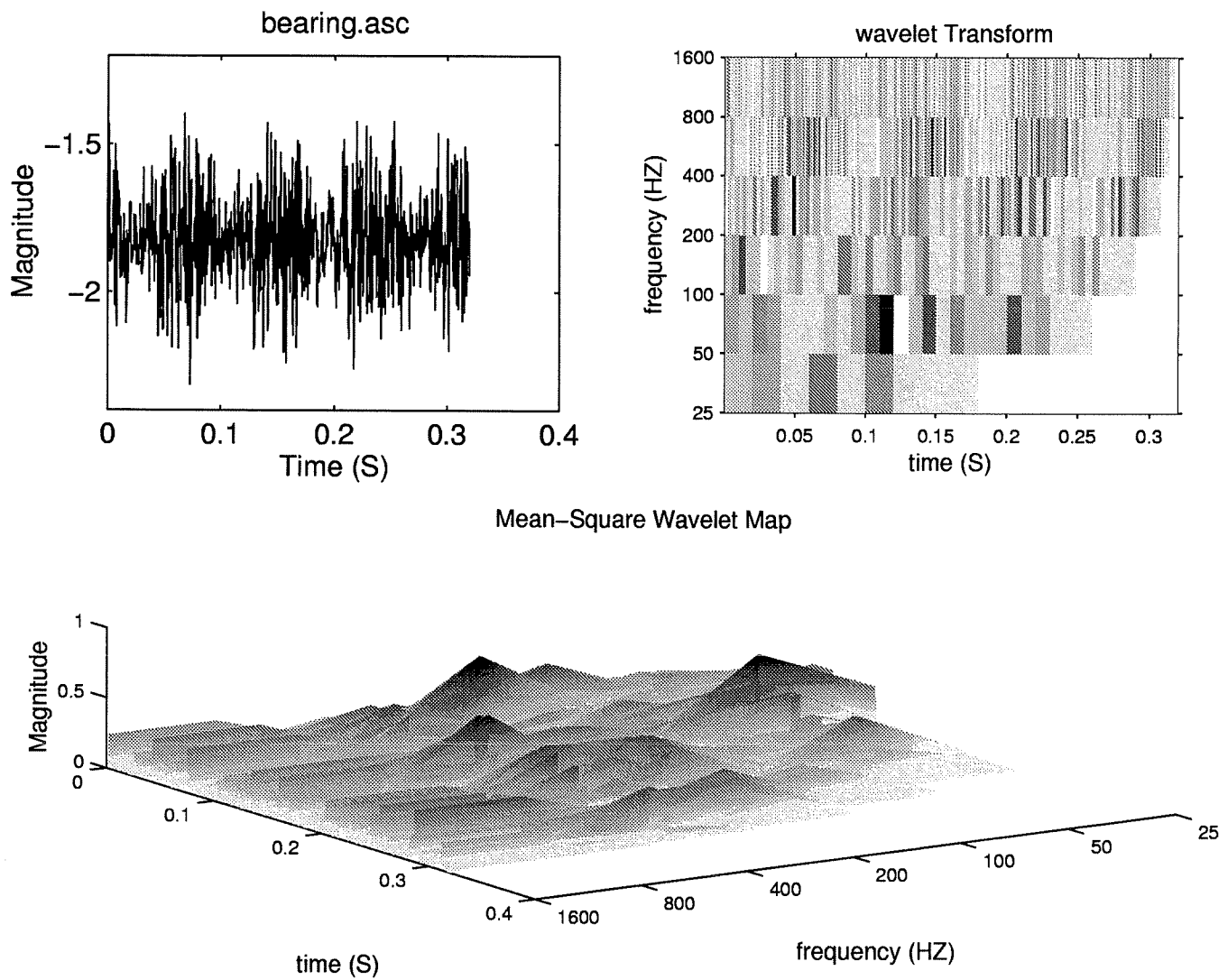


Figure 25: Wavelet transform and mean-square wavelet map of the measured signal on a defective bearing.

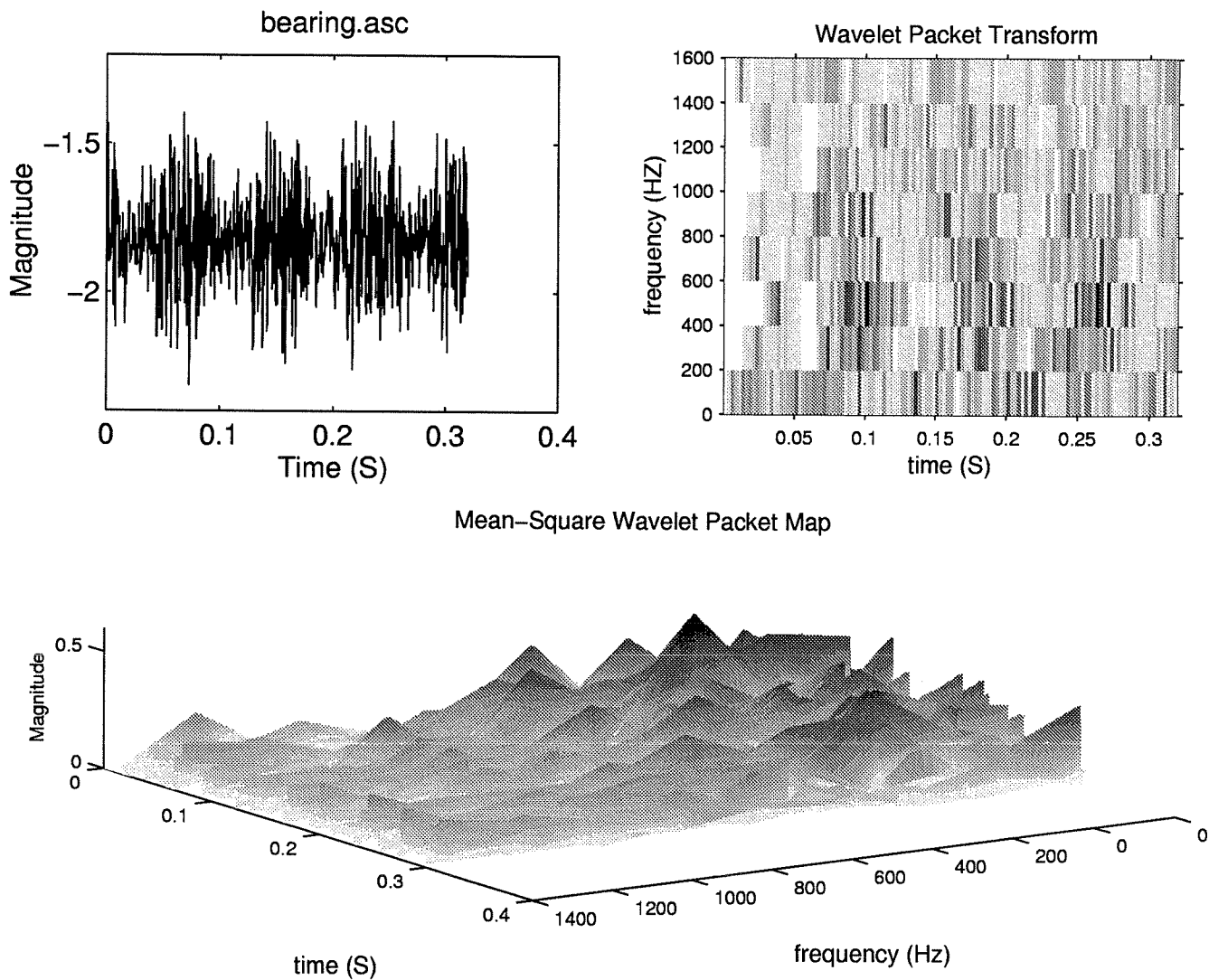


Figure 26: Wavelet packet transform and mean-square wavelet packet map of the measured signal on a defective bearing.

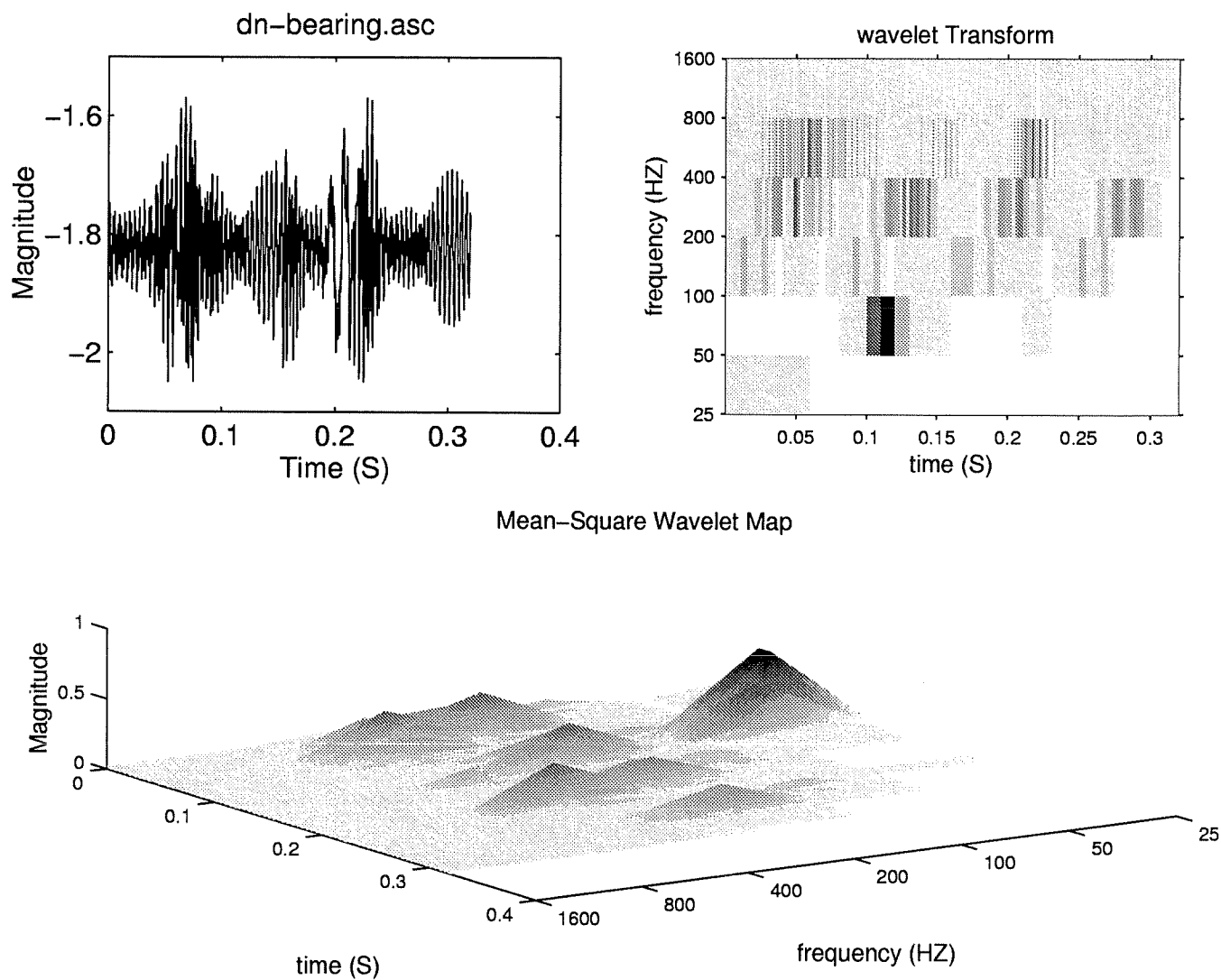


Figure 27: Wavelet transform and mean-square wavelet map of the de-noised signal of the defective bearing.

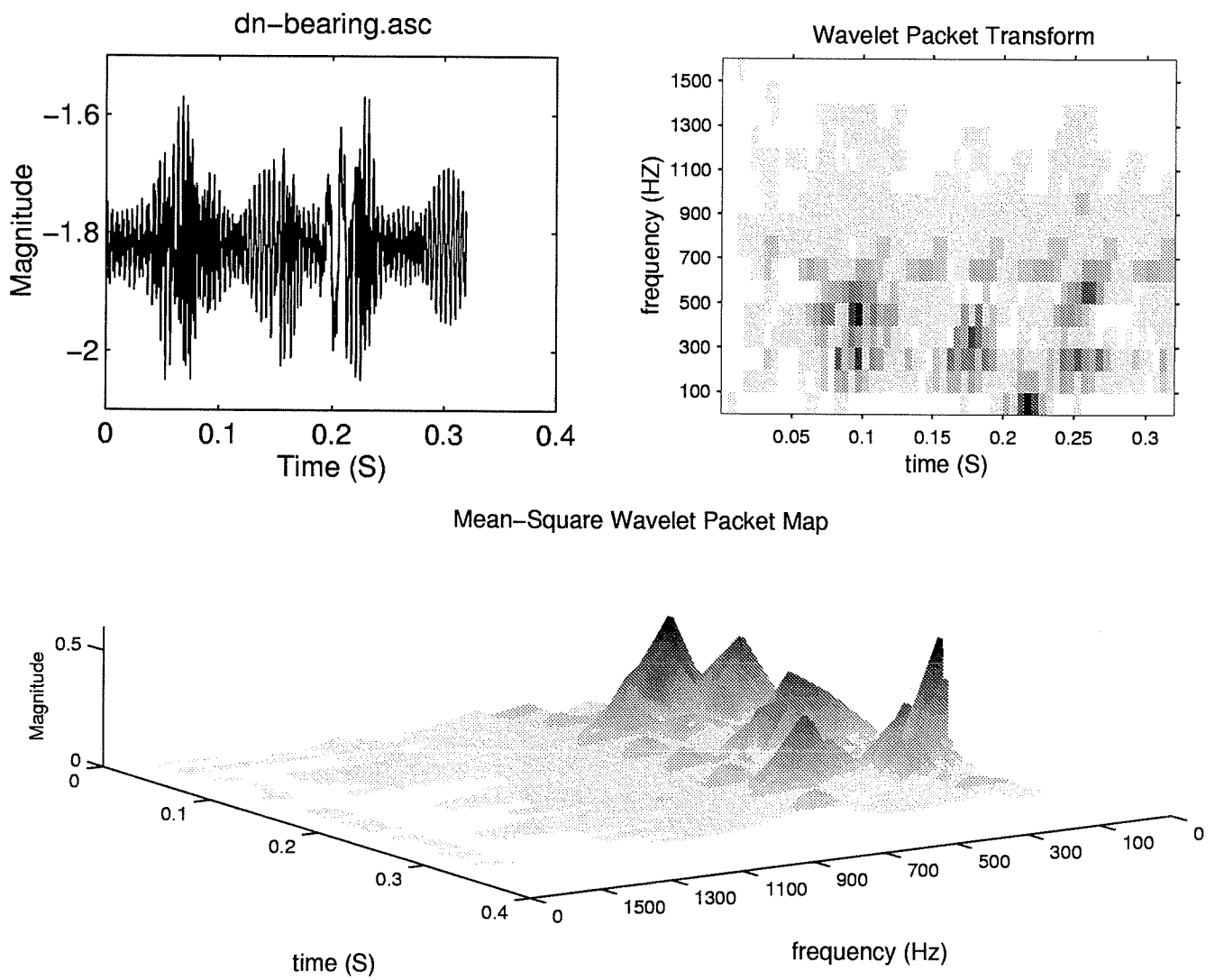


Figure 28: Wavelet packet transform and mean-square wavelet packet map of the de-noised signal of the defective bearing.

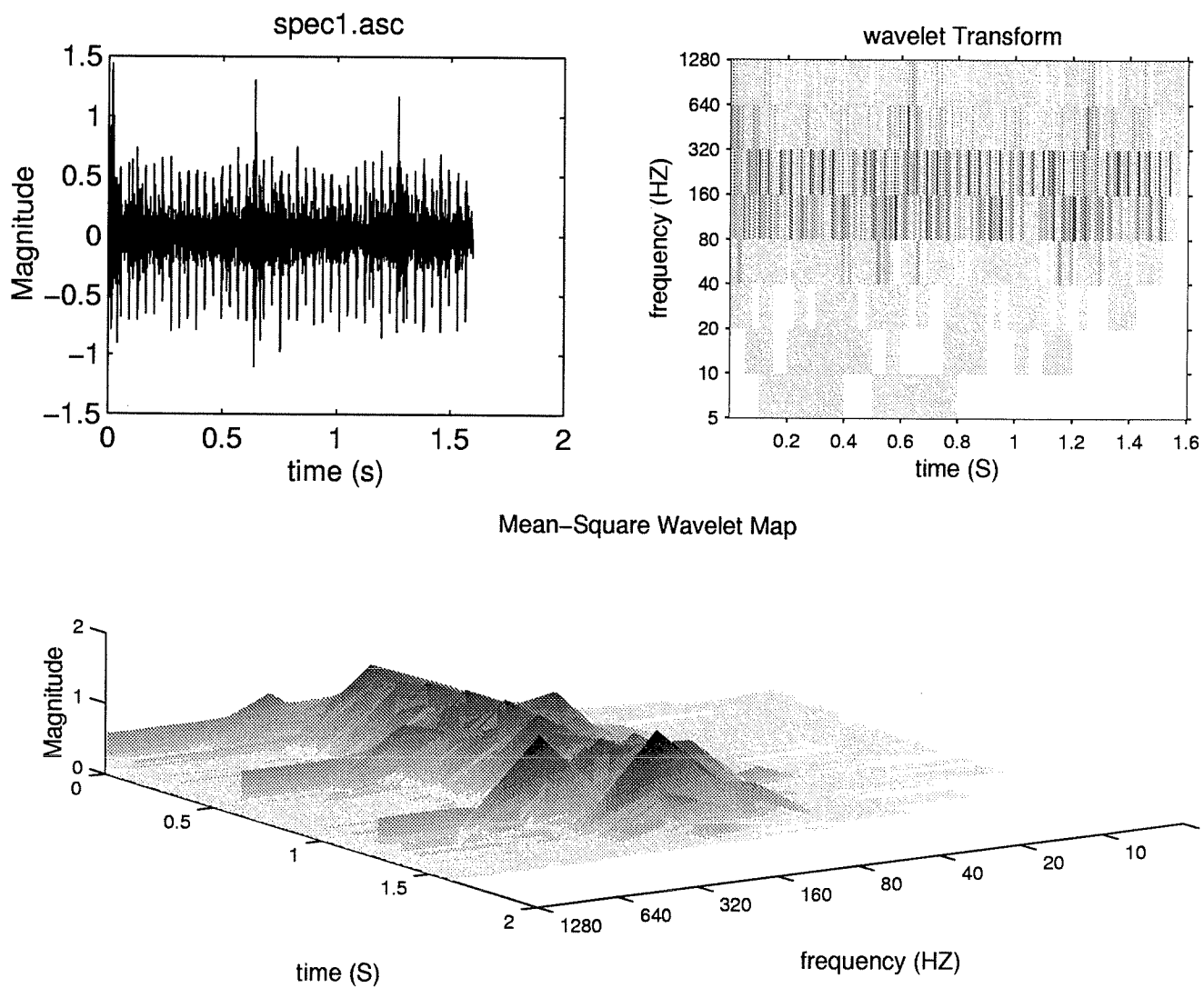


Figure 29: Wavelet transform and mean-square wavelet map of the signal measured on a defective gearbox.

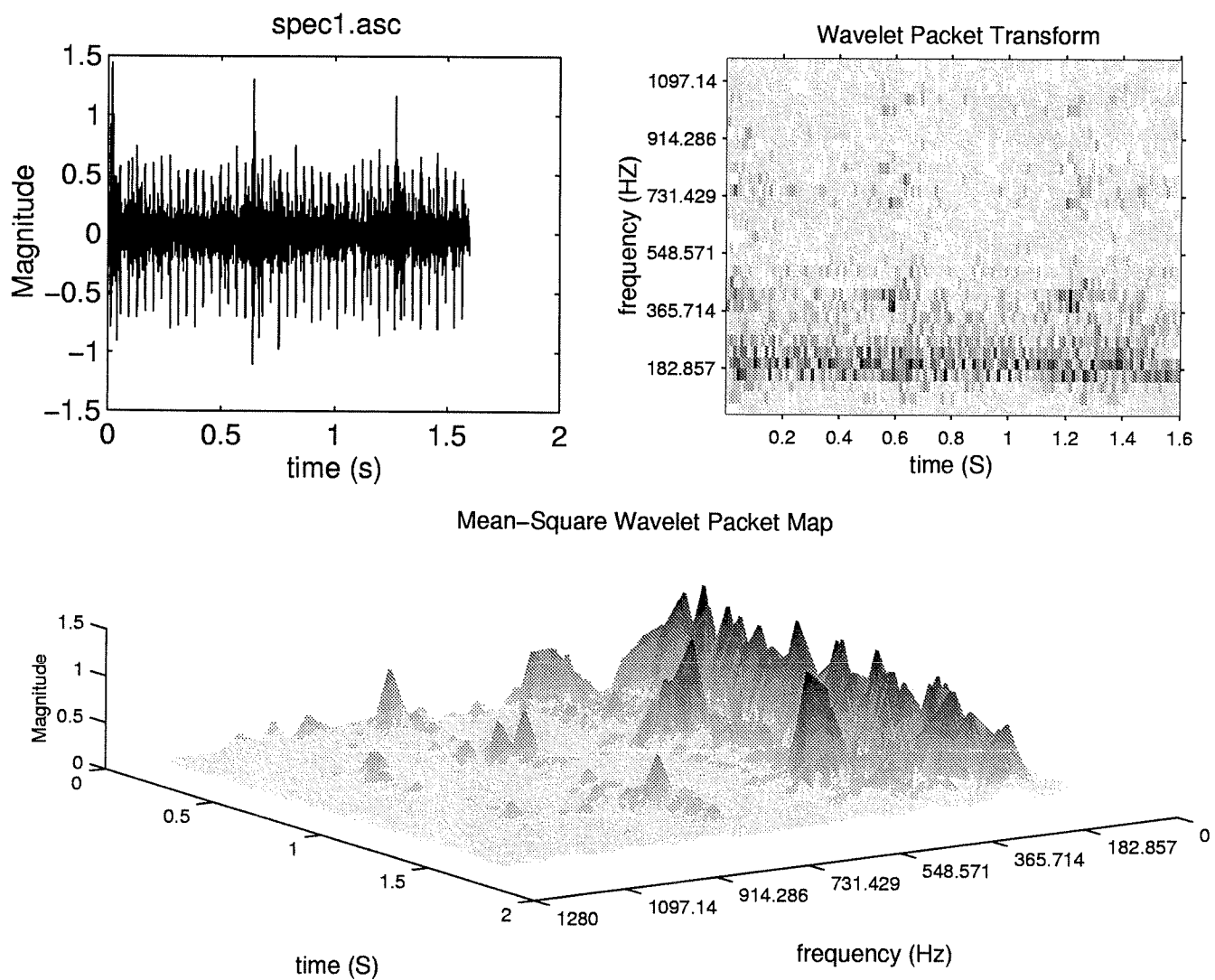


Figure 30: Wavelet packet transform and mean-square wavelet packet map of the signal measured on a defective gearbox.

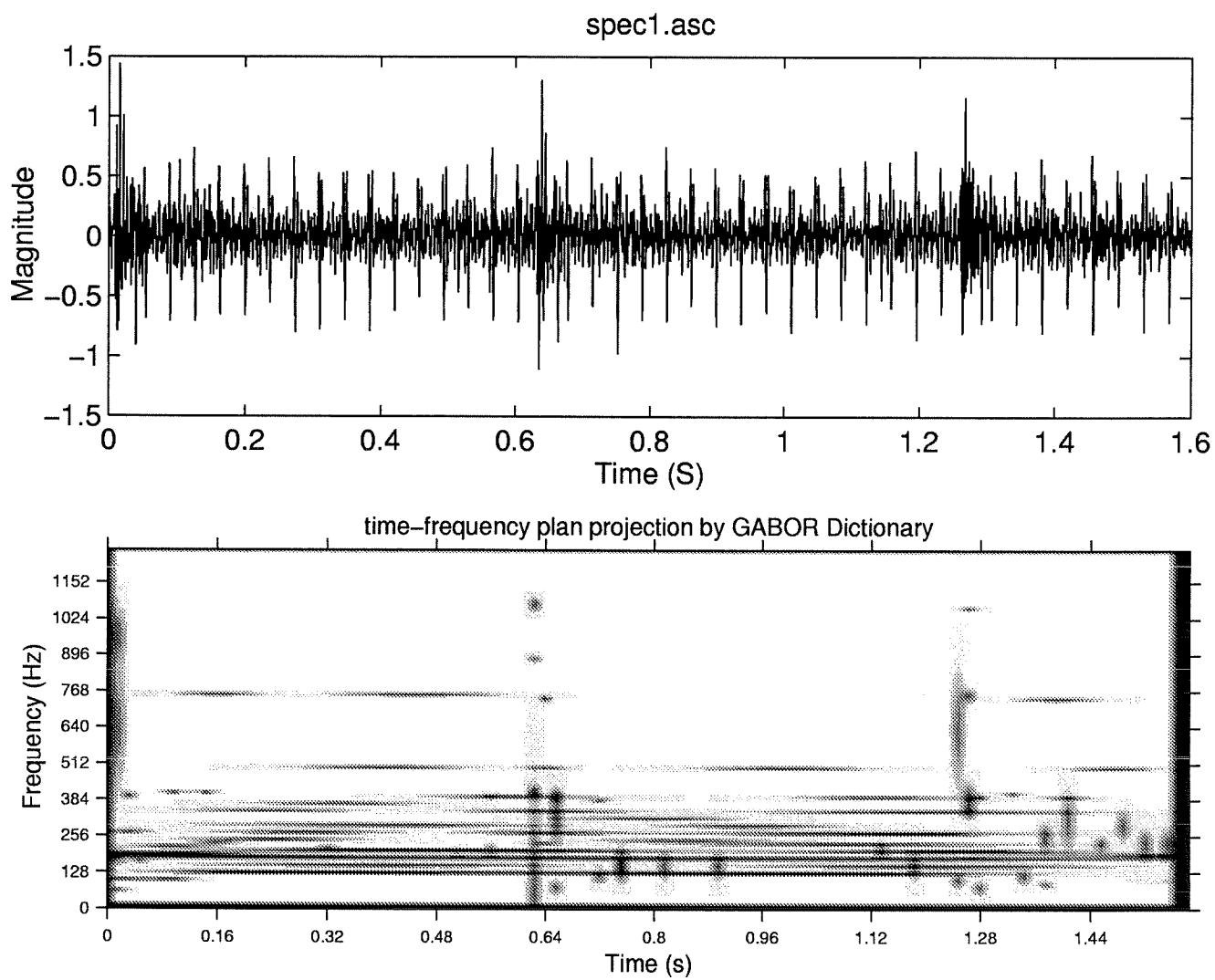


Figure 31: Time-frequency representation of the signal measured on a defective gearbox by the Gabor dictionary.

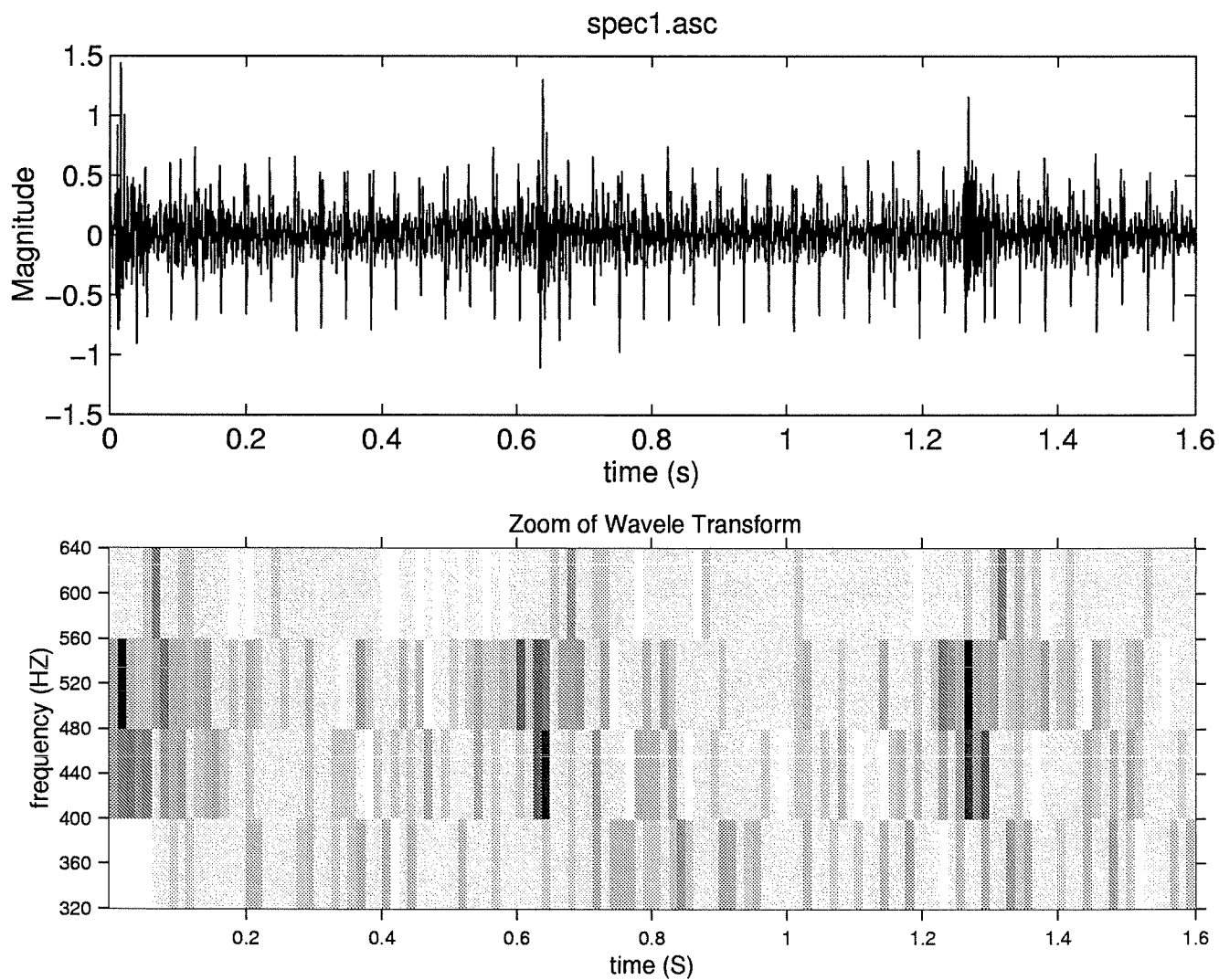


Figure 32: Zoom in wavelet transform of the signal measured on a defective gearbox between the frequency band 320 Hz and 640 Hz.

ÉCOLE POLYTECHNIQUE DE MONTRÉAL



3 9334 00227627 5

École Polytechnique de Montréal
C.P. 6079, Succ. Centre-ville
Montréal (Québec)
H3C 3A7